



OPEN

## Early breast cancer detection via infrared thermography using a CNN enhanced with particle swarm optimization

Riyadh M. Alzahrani<sup>1</sup>, Mohamed Yacin Sikkandar<sup>1</sup>✉, S. Sabarunisha Begum<sup>2</sup>, Ahmed Farag Salem Babat<sup>3</sup>, Maryam Alhashim<sup>4</sup>, Abdulrahman Alduraywish<sup>1</sup>, N. B. Prakash<sup>5</sup> & Eddie Y. K. Ng<sup>6</sup>

Breast cancer remains the most prevalent cause of cancer-related mortality among women worldwide, with an estimated incidence exceeding 500,000 new cases annually. Timely diagnosis is vital for enhancing therapeutic outcomes and increasing survival probabilities. Although conventional diagnostic tools such as mammography are widely used and generally effective, they are often invasive, costly, and exhibit reduced efficacy in patients with dense breast tissue. Infrared thermography, by contrast, offers a non-invasive and economical alternative; however, its clinical adoption has been limited, largely due to difficulties in accurate thermal image interpretation and the suboptimal tuning of machine learning algorithms. To overcome these limitations, this study proposes an automated classification framework that employs convolutional neural networks (CNNs) for distinguishing between malignant and benign thermographic breast images. An Enhanced Particle Swarm Optimization (EPSO) algorithm is integrated to automatically fine-tune CNN hyperparameters, thereby minimizing manual effort and enhancing computational efficiency. The methodology also incorporates advanced image preprocessing techniques—including Mamdani fuzzy logic-based edge detection, Contrast-Limited Adaptive Histogram Equalization (CLAHE) for contrast enhancement, and median filtering for noise suppression—to bolster classification performance. The proposed model achieves a superior classification accuracy of 98.8%, significantly outperforming conventional CNN implementations in terms of both computational speed and predictive accuracy. These findings suggest that the developed system holds substantial potential for early, reliable, and cost-effective breast cancer screening in real-world clinical environments.

**Keywords** Breast cancer, Generative adversarial network, Optimization techniques, Type-2 fuzzy logic approach, Hyperparameters tuning

Breast cancer is recognized as the second leading cause of mortality among women worldwide<sup>1</sup>. Early detection and timely intervention are critical in reducing breast cancer-related deaths. Advances in current technologies and data mining methodologies have significantly enhanced the capabilities of medical systems in analyzing, predicting, and accurately classifying cancer cases<sup>2</sup>. Breast cancer originates from the abnormal proliferation of cells within breast tissue, leading to the formation of various types of lesions. These lesions are typically characterized by asymmetries between the left and right breasts, disruption of normal tissue architecture, the presence of micro-calcifications (MCs), and masses of differing shapes and sizes<sup>3</sup>. Mammography, which involves the radiological examination of breast tissue in conjunction with physical assessment, serves as an effective screening tool for early detection of breast cancer. Its implementation has led to a 42% reduction in breast cancer mortality since 1989<sup>4</sup>. Importantly, approximately 95% of breast cancer cases are currently diagnosed at

<sup>1</sup>Department of Medical Equipment Technology, College of Applied Medical Sciences, Majmaah University, Al Majmaah 11952, Saudi Arabia. <sup>2</sup>Department of Biotechnology, P.S.R. Engineering College, Sivakasi 626140, India.

<sup>3</sup>Dr. Mohammad Alfagih Hospital, Riyadh 13223, Saudi Arabia. <sup>4</sup>Department of Radiology, College of Medicine, Imam Abdulrahman Bin Faisal University, Dammam 34212, Saudi Arabia. <sup>5</sup>Department of Electrical and Electronics Engineering, National Engineering College, Kovilpatti 628503, Tamilnadu, India. <sup>6</sup>School of Mechanical & Aerospace Engineering, College of Engineering, Nanyang Technological University, Singapore 639798, Singapore. ✉email: m.sikkandar@mu.edu.sa

an early stage<sup>5</sup>. With the exponential increase in oncology-related data, data science and machine learning (ML) techniques have gained substantial attention as powerful tools to address diverse clinical challenges<sup>6,7</sup>. Unlike conventional programming paradigms that rely on explicitly defined instructions, ML algorithms learn patterns directly from data by mapping mathematical functions to inputs for predictive or classification purposes<sup>8</sup>.

Traditional artificial intelligence (AI) methods such as Support Vector Machines (SVM) and Random Forest (RF) have demonstrated notable success in classifying breast cancer into triple-negative and non-triple-negative subtypes, predicting metastatic progression, and identifying early recurrence of the disease<sup>9</sup>. Moreover, advanced ensemble learning algorithms such as Gradient Boosted Trees and eXtreme Gradient Boosting (XGBoost) have been effectively employed to predict metastasis in breast cancer and survival outcomes in epithelial ovarian cancer, respectively<sup>10,11</sup>. Recent developments in machine learning have incorporated deep learning and radiomics to classify breast cancer using radiological imaging and histopathological slides, achieving superior performance across multiple benchmarks<sup>12–14</sup>. These methodologies, integrated with advancements in data acquisition and processing technologies, have significantly enhanced the ability to handle high-dimensional data—enabling effective data classification, visualization, and interpretation.

Furthermore, the combination of robust feature extraction and high-quality datasets with AI-driven techniques contributes to the development of reliable decision support systems for clinicians, effectively reducing diagnostic bias<sup>15–18</sup>. Comparative analyses using various machine learning and visualization approaches—including k-Nearest Neighbors (k-NN), Logistic Regression, Naïve Bayes, SVM, Decision Trees, Rotation Forests, and Random Forests—have been performed for breast cancer detection and diagnosis<sup>15</sup>. These studies, particularly those employing the Wisconsin Breast Cancer dataset with 32 distinct features, revealed that Logistic Regression yielded the highest classification accuracy among all tested models. This was primarily due to its computational efficiency and ease of training. Additionally, Wakili et al. (2022) proposed a homogeneous ensemble model leveraging a Multilayer Perceptron (MLP) architecture, which also demonstrated promising results in breast cancer classification tasks<sup>16</sup>.

Compared to Genetic Algorithm (GA) and Particle Swarm Optimization (PSO), the performance of the Multilayer Perceptron (MLP) has shown notable improvement when its parameters are optimized using the Orthogonal Design of Experiments with Model Averaging (ODMA) approach. A similar strategy for effective feature selection and parameter tuning in Artificial Neural Networks (ANNs) was proposed by Heenaye et al. (2021), who integrated Artificial Immune Systems with a breast cancer detection model based on the Artificial Bee Colony algorithm<sup>17</sup>. This hybrid model employed Momentum-based Gradient Descent Backpropagation and utilized Simulated Annealing to enhance local search capabilities. It demonstrated strong classification capabilities, achieving accuracy exceeding 99%. In a big data context, Sakri et al. (2018) developed a breast cancer detection model using an optimized ANN framework<sup>18</sup>. The model incorporated a modified Dragonfly Algorithm for feature selection and utilized the Grey Wolf Optimization algorithm for ANN parameter tuning. The classification was based on selected features from the Wisconsin Breast Cancer dataset. However, while the model showed promise, the use of a more advanced classification technique could potentially yield even higher accuracy. Mohan et al. (2013) proposed a breast cancer classification model leveraging feature selection through Whale Optimization and ensemble classification using highly randomized trees<sup>19</sup>. Despite its potential, a significant limitation was observed: the random initialization of hyperparameters in the optimization phase occasionally resulted in reduced model efficiency. On the image enhancement front, histogram-based enhancement techniques have been widely explored. Ibrahim et al. (2023) presented a PSO-based method for tuning the enhancement parameters of Contrast Limited Adaptive Histogram Equalization (CLAHE), which incorporated Local Contrast Modification (LCM). Their study concluded that the PSO-optimized LCM-CLAHE method significantly outperformed existing techniques, producing superior-quality mammographic images<sup>20</sup>.

CNNs have demonstrated exceptional capabilities in addressing complex challenges associated with medical image classification, including the detection of Alzheimer's disease, retinal disorders, MRI abnormalities, and breast cancer. Typically, CNN parameters are fine-tuned through automated learning during the training phase. However, determining the optimal set of parameters remains a significant challenge due to the vastness and complexity of the hyperparameter search space, which often leads to suboptimal configurations. As a result, researchers frequently encounter difficulties in identifying the most suitable parameter values for achieving optimal model performance. Despite the inherent optimization mechanisms within CNNs, these do not necessarily guarantee convergence to a global optimum. Therefore, the process of hyperparameter tuning often involves extensive trial-and-error procedures and reliance on expert domain knowledge. This limitation significantly hinders the effective deployment of CNN-based solutions in real-world medical applications, particularly in the analysis of MRI images<sup>6</sup>. The remainder of this article is structured as follows: Section II provides a comprehensive review of the literature, highlights the limitations of existing methods, and outlines the motivation and objectives of the current research on breast cancer classification. Section III details the materials and methods used in the study. Section IV presents the proposed methodology, including a block diagram and a step-by-step explanation of the associated processes. Section V discusses the experimental results and analysis, while Section VI concludes the paper and suggests directions for future research.

## Literature review

### Existing methods in breast Cancer detection

Traditional breast cancer detection methods, such as mammography, ultrasound, and biopsy, have been the standard for years. While these methods are effective, they often involve invasive procedures (e.g., biopsy) or require physical contact (e.g., mammography), which can cause discomfort to patients. Moreover, these methods are not always accessible due to high costs, and mammography, in particular, is less effective in women with dense breast tissue. As a result, there is a growing interest in alternative non-invasive methods, such as thermographic imaging, which offers the potential for early detection without the need for physical contact.

### Limitations of current thermographic imaging approaches

Thermographic imaging, though non-invasive and cost-effective, faces significant challenges when used for breast cancer detection. One of the key limitations is the difficulty in extracting meaningful features from thermal images that can accurately distinguish between cancerous and non-cancerous tissue. Conventional image processing techniques, such as thresholding or basic edge detection, often fail to handle the complexity of thermal patterns in breast tissue, resulting in poor accuracy and high false-positive rates.

Additionally, many existing systems rely on basic machine learning techniques or standard convolutional neural networks (CNNs), which, while powerful, require manual tuning of hyperparameters—a process that is both time-consuming and prone to human error. Traditional optimization methods, such as grid search or random search, are often computationally expensive and do not guarantee optimal results. This makes it challenging to deploy reliable, high-performance models in clinical settings, where speed and accuracy are critical.

The above methods are insufficient while thermographic imaging holds promise, its practical application in breast cancer detection has been hindered by the limitations of existing methods. Basic image processing techniques often fail to capture the subtle thermal variations necessary for accurate classification. Additionally, the reliance on manual or conventional optimization techniques to tune deep learning models reduces the efficiency of current systems and leads to suboptimal performance.

In<sup>6,11,21</sup>, thermography patterns were fed as input to the training algorithm in medical image applications. The major drawback of the above-mentioned approaches was the pre-processing step of data before feature extraction. They commonly used filters, gray scale image conversion and cropping of patterns were proposed. These techniques failed to extract high level features from the pattern, which may cause a reduction in efficiency of the recognition. Accurate diagnosis of BC is the most important step for treatment. Whale optimization can be used to reduce the dimensionality of the dataset and extract the pertinent features required for precise classification. When the analysis was conducted using the Wisconsin BC diagnostic data set, the model achieved an accuracy rate of more than 99%. A similar process was used by Kamel et al., (2019), with the exception that the SVM classifier was used to classify BC data and gray-wolf optimization was used to select features<sup>22</sup>. The major drawback behind the algorithm is that the use of MCSVM causes high computation time and algorithm suffers from overfitting problems. Three of the eight classifiers used for ensemble classification using a voting mechanism were SVM learning with stochastics gradient de-scent optimizations, MLP, and common logistic regression learning. The classifiers' performances were assessed using both hard and soft voting procedures. A machine learning-driven cloud-based BC diagnostic system was created Lahoura et al., (2021) and they used the Wisconsin Diagnostic BC data set to assess the model<sup>23</sup>. The gain ratio approach was used in the feature selection process to weed out features that weren't necessary. Recently, Jakhar et al., (2024) developed a stacked-based ensemble learning framework called SELF was introduced to classify BC early on using histological pictures of tumor cells and computer-aided diagnosis tools. In this model, the stacking ensemble technique was applied<sup>24</sup>. The basic learners were defined as Random Forest, Extra Tree, Adaboost, KNN, and Gradient Boosting classifiers. The last estimator was the logistic regression model. They failed to hybrid the appropriate ML and DL approach for recognizing the type of breast cancer.

Techniques based on machine learning (ML) have demonstrated excellent performance for various image recognition tasks<sup>25</sup>. Because of its excellent discriminating ability, SVM is frequently used to solve classification problems<sup>26</sup>. Researchers are continuously trying to develop new machine learning-based systems to detect breast cancer at its early stages. The key differences among these studies lie in the choice of machine learning models, the mammography datasets utilized, and the feature extraction methods employed. Most published works have employed Support Vector Machine (SVM) as a classifier, which is assessed using different subsets of the Mammographic Image Analysis Society (MIAS) or the Digital Database for Screening Mammography (DDSM) databases.

Görgel et al., (2013) reported an accuracy of 94% using a local seed growing technique combined with spherical wavelet transformation and SVM classifier for mass/non-mass classification<sup>27</sup>. Iqbal et al., (2022) used Gabor filters with different scales and directions, and the result was 0.98 area under ROC<sup>28</sup>. Berbar et al., (2012) reported accuracy rates of 98.63% and 97.25% with SVM and k-NN, respectively, by utilizing hybrid features based on statistical measures and local binary patterns<sup>29</sup>. Mukhmetov et al., (2023) introduced a new Physics-Informed Neural Network (PINN) approach designed for rapid forward simulations of heat transfer in breast cancer models<sup>30</sup>. These results offer significant potential for creating a non-invasive and safer alternative to traditional breast self-examination methods like mammography. For artificial generation of dataset to balance the CNN architecture training process GAN is used in this proposed work. But still Generation of accurate image as from databases is a challenge task and that can be hybrid with some more architecture and make the discriminator fool for collecting artificial databases. Computation time can be minimized by using various batch normalization algorithms. Edge detection is crucial in breast cancer tumor identification because it highlights the boundaries of abnormal growth, allowing for precise localization and measurement of tumors. This helps in distinguishing malignant masses from surrounding tissues in medical images like mammograms or MRIs, enhancing diagnostic accuracy. Furthermore, accurate edge detection supports advanced algorithms in automating tumor segmentation, aiding in early detection and treatment planning. Choosing an appropriate edge detection algorithm for recognizing breast cancer in thermography images is paramount. However, optimizing deep learning architectures results in longer training times and requires substantial memory storage. Here it is proposed to use advanced techniques for edge detection and further classification and is described in the next section.

Furthermore, existing systems often struggle with computational efficiency, leading to longer processing times that are not suitable for real-time clinical diagnostics. As a result, these methods are insufficient in providing the speed, accuracy, and reliability needed for widespread use in clinical practice.

This research work introduces a novel solution to the above challenges by utilizing an Enhanced Particle Swarm Optimization (EPSO) algorithm to automatically optimize the hyperparameters of convolutional neural networks (CNNs). EPSO eliminates the need for manual tuning, providing an efficient way to identify optimal hyperparameters, which accelerates model performance and enhances accuracy. Additionally, the integration of advanced image processing techniques—such as Mamdani fuzzy logic for edge detection, CLAHE for contrast enhancement, and a median filter for noise reduction—improves the ability to capture fine thermal details, leading to more accurate classification of breast tissue.

By addressing both the optimization and image processing challenges, this research work provides a more reliable, faster, and clinically viable solution for breast cancer detection using infrared thermography.

### **Hyperparameter optimization and deep learning in Cancer research**

The optimization of hyperparameters is a critical component of training robust and efficient deep learning models. In cancer detection tasks, particularly in the classification of breast cancer, the role of hyperparameter tuning becomes even more significant as it directly impacts the model's ability to generalize and accurately classify pathological conditions. Particle Swarm Optimization (PSO) has emerged as one of the prominent techniques for optimizing hyperparameters in deep learning models due to its simplicity and effectiveness in navigating complex, high-dimensional search spaces.

Recent studies have explored the effectiveness of various hyperparameter optimization techniques in improving the performance of deep learning models in cancer research. Wang et al. (2022) demonstrated the use of hyperparameter optimization to enhance the performance of machine learning models in cancer prognosis, highlighting the importance of fine-tuning learning rates, batch sizes, and network architectures for accurate cancer detection (Wang et al., 2022). Similarly, Choi et al. (2023) presented a comparison of several optimization algorithms, including PSO, for hyperparameter tuning in cancer classification tasks. The study underscored how PSO, when applied to convolutional neural networks (CNNs), significantly improved classification accuracy in identifying malignant tumor cells in medical images (Choi et al., 2023). Furthermore, Patel et al. (2024) explored the use of PSO for optimizing the CNN model used for early-stage cancer detection. The optimization of hyperparameters such as convolutional kernel size, dropout rates, and learning rates contributed to the significant reduction in false positive rates, providing a more reliable diagnostic tool for clinicians (Patel et al., 2024). As deep learning continues to revolutionize medical imaging and cancer detection, several studies, including Liu et al. (2023), have investigated the use of more complex optimization strategies like Bayesian optimization and genetic algorithms, alongside PSO, to fine-tune deep learning models. Their findings indicate that these optimization techniques improve model robustness, which is crucial when developing systems for medical decision support (Liu et al., 2023). Additionally, Shuwei et al. (2024) discussed how integrating PSO with advanced CNN architectures can substantially enhance the performance of automated breast cancer detection systems. Their results demonstrated an increase in diagnostic accuracy, emphasizing the complementary role of optimization algorithms in medical deep learning models<sup>30</sup>. These studies underscore the significance of hyperparameter optimization in the development of deep learning models for cancer diagnosis. By employing PSO to optimize CNN models in this study, it is aimed to harness the strengths of both CNN architecture and optimization algorithms to achieve superior performance in breast cancer classification.

### **Research gaps**

Despite the advances in early breast cancer detection, traditional diagnostic methods like mammography often require physical contact, are invasive, and may not be accessible in all regions due to cost and infrastructure limitations. Thermographic imaging, while promising, has not been fully utilized in automated systems for breast cancer classification due to challenges in image processing, accuracy, and the complexity of optimizing machine learning models. Furthermore, existing deep learning models for thermographic image classification often rely on traditional optimization techniques that require extensive manual tuning of hyperparameters, which is both time-consuming and resource intensive.

### **Materials and methods**

The breast thermal images used in this study were from the Database for Mastology Research, managed by Antonio Pedro University Hospital (HUAP) in Brazil. This dataset contains infrared thermographic images of breast tissue, specifically collected for breast cancer (BC) detection research. The data was publicly available for access between 15 February 2024 and 15 August 2024<sup>31,32</sup>. Image acquisition was done with Infrared camera FLIR SC-620, with a resolution of 640 × 480: pixel = 45 μm. The dataset consists of 82 patients and 7909 thermography images of BC. Images of both benign and malignant cases are included in this dataset.

### **Patient demographics**

The dataset consists of breast thermal images from both healthy individuals **and** patients with diagnosed breast cancer. The dataset includes a variety of patient profiles to ensure diversity and robustness for research purposes. The patient demographic information includes:

- Age Range: The dataset includes patients aged between 20 and 80 years.
- Gender: All images are from female patients, as the dataset specifically focuses on breast cancer detection in women.
- Health Status: The dataset contains both normal (non-cancerous) breast thermal images and images of patients diagnosed with various stages of breast cancer.

## Inclusion and exclusion criteria

- Inclusion Criteria:** The images included in the dataset are from patients diagnosed with breast cancer, as well as healthy controls. All images were collected from patients who had undergone thermographic scans as part of routine clinical assessments at HUAP.
- Exclusion Criteria:** Images from patients with incomplete clinical records, those who underwent non-standard imaging procedures, or those with other unrelated health conditions (e.g., active infections or inflammatory diseases affecting the breast area) were excluded from the dataset.

The dataset can be accessed at the following URL: <https://visual.ic.uff.br/dmi/prontuario/home.php>.

## Proposed work

This study addresses these gaps by proposing an automated system that utilizes infrared thermography for non-invasive, cost-effective breast cancer detection. The key innovation of this work lies in the introduction of an Enhanced Particle Swarm Optimization (EPSO) algorithm, which efficiently identifies optimal CNN hyperparameters, reducing the manual intervention required for model tuning and improving computational efficiency. Additionally, the integration of advanced image processing techniques—such as Mamdani fuzzy logic for edge detection, CLAHE for contrast enhancement, and a median filter for noise reduction—enhances diagnostic accuracy. By combining these novel approaches, our method not only improves the classification accuracy but also accelerates the detection process, offering a viable solution to the limitations of current thermographic detection systems.

Generally, enhanced particle swarm optimization (EPSO) can be clustered into three groups namely, PSO parameters, structure of CNN, Training options. In the first group, the EPSO algorithm consists of the following four parameters: Quantity of repetitions, quantity of populace, social coefficient and cognitive coefficient. With separate initialization, the proposed work was carried out to perform consistent concert. In addition to that, Quantity of Populace determines the particles working in EPSO algorithm. Social and Cognitive Coefficient performs how fast the particle reaches the global position. In the proposed approach, a higher coefficient value in EPSO facilitates faster convergence to the global optimum with reduced computational time and lower population diversity. In the second group, the CNN architecture determines the range and values of five different parameters: Quantity of layers, Quantity of Neurons in FC layer, Size of Convolution Kernel, Pooling Kernel Size and Stride Size. Initial and foremost step in the projected work is to generate the preliminary swarm for designing the structure of CNN. This preliminary swarm will cover entities with structures selected at chance restricted by these limits. The depth of the CNN structure will be determined by the Quantity of layers. The above said ranges and values are commonly used to design a user defined CNN architecture. Once the architecture is designed, the optimization approach can alter the number of layers based on our research problem. The proposed work is performed in the Nvidia Tesla P50 Graphics Processing Unit with 16 GB of memory system. Figure 1 represents

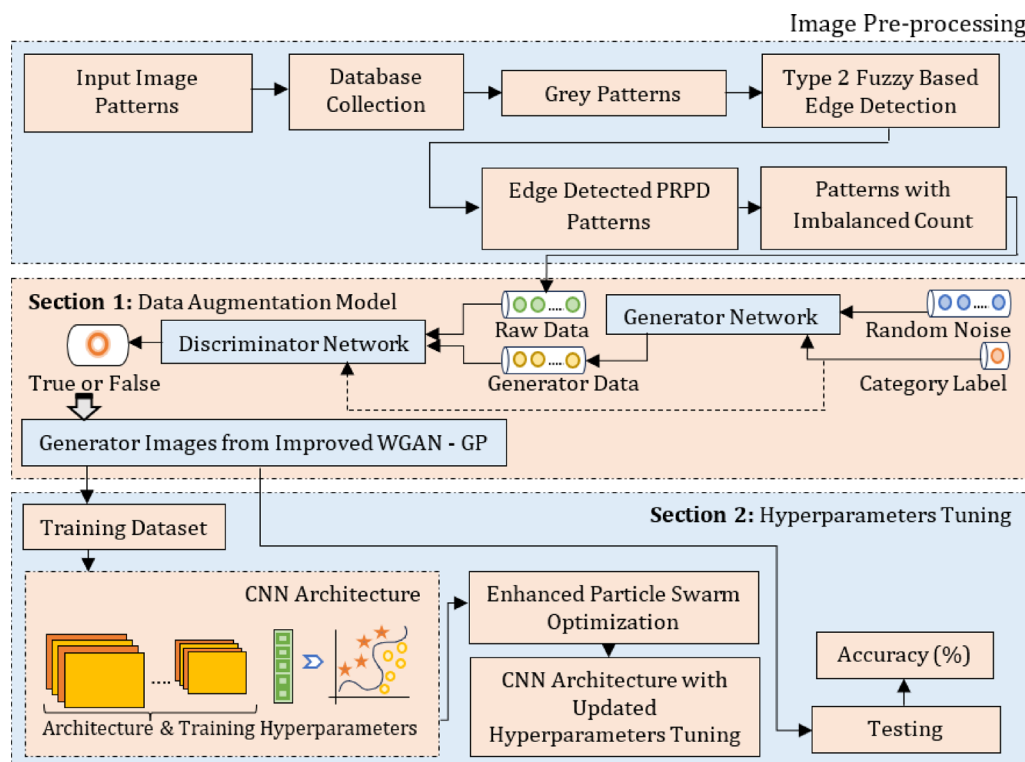


**Fig. 1.** Proposed EPSO with EGAN Algorithm for Breast cancer recognition.

the proposed work, initially pre-processing plays a major role in database management station. Next to that, GAN is used to generate artificial images with low penalty gradient rate. And at last optimized CNN architecture is used to recognition the breast cancer.

In the third group, the training options in CNN architecture are gritty for each BO. This group contains five parameters related to training options: Activation function, Learning rate, Dropout rate, Epochs for particle estimation and Epochs for best CNN. The main function of the above said parameters is to compute particles during weight updating process. Quantity of epochs determines how the network is trained for input dataset based on evaluating the training accuracy. The global best value from the optimization algorithm is declared as best value for the CNN parameters is computed in the testing dataset. During training process to avoid the overfitting problem dropout parameter. These dropping proportion estimates the connection amid the neurons in the FC layer.

#### Summary of the CNN Architecture:

Layer Type	Output Size	Activation Function
Input Layer	$224 \times 224 \times 3$	-
Convolutional Layer 1	$224 \times 224 \times 32$	ReLU
Convolutional Layer 2	$224 \times 224 \times 64$	ReLU
Convolutional Layer 3	$224 \times 224 \times 128$	ReLU
Max Pooling Layer 1	$112 \times 112 \times 128$	-
Max Pooling Layer 2	$56 \times 56 \times 128$	-
Fully Connected Layer 1	512	ReLU
Fully Connected Layer 2	128	ReLU
Output Layer	10	Softmax

#### Notes:

- The **input images** are resized to  $224 \times 224$  before being fed into the network.
- The **convolutional layers** progressively extract more complex features from the images.
- Max pooling layers** help reduce the spatial dimensions and computational cost while maintaining essential information.
- Fully connected layers** combine the features extracted by the convolutional layers and make the final predictions.
- The **dropout layers** help regularize the model and prevent overfitting by randomly setting some of the weights to zero during training.
- Softmax activation** in the output layer ensures that the model outputs a probability distribution over the 10 possible classes (abnormal conditions).

#### Pre-processing of patterns using edge detection techniques

Using simple kernels or operators, early monoscale methods like the Sobel method<sup>6</sup> yield the edge strength maps. Despite their effectiveness, these early methods were sensitive to noise, which is why some monoscale algorithms employ kernels of varying sizes<sup>21</sup>. uses the Laplacian of Gaussian kernels to generate the edge response. By changing the kernel size, one can apply the Laplacian of Gaussian kernels to thin or wide edges. The more advanced method for edge detection that has gained the most traction is the canny detector. The current differentiation-based edge detection algorithms mainly use first- or second-order derivatives of an image's light intensity with one or more scales to identify edge contours in images. Since Russo<sup>33</sup> introduced fuzzy inference as a useful method for extracting edge features with strong noise robustness, the application of fuzzy theory in edge detection has gained more and more attention. The module of Type 2 fuzzy has been demonstrated in Fig. 2.

Fuzzy theory aids in the recognition of edge structures because edge definitions in images are inherently uncertain. An edge detector that tackles edge detection problems for grey-level images with uncertainty, imprecision, or both was proposed by Versaci and Morabito<sup>34</sup>. The combined use of fuzzy entropy minimization

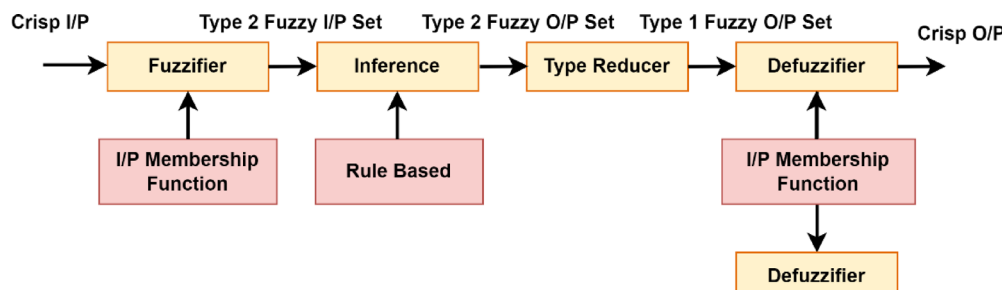


**Fig. 2.** Type 2 Fuzzy Edge Detection Module.

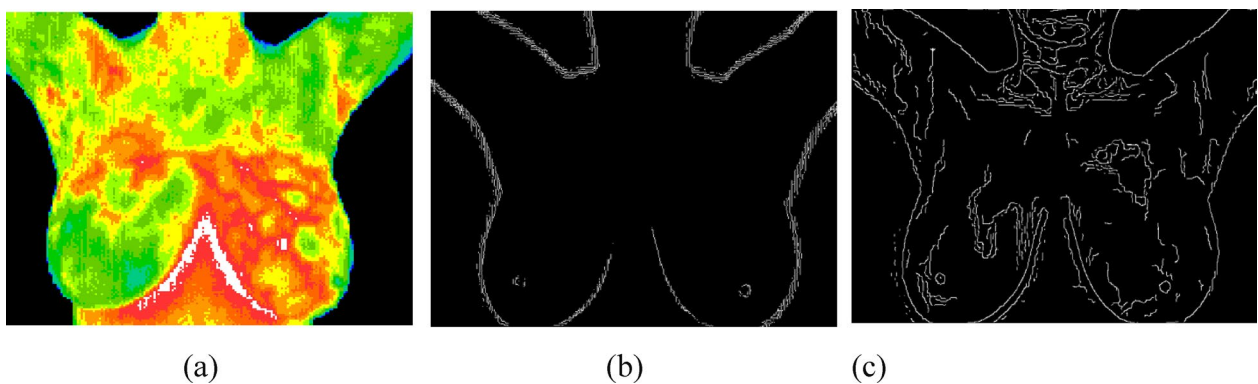


**Fig. 3.** Edge Detected breast image with cancer. (a) Input raw Image; (b) Canny Edge detected image; (c) Type 2 Fuzzy edge detected image.

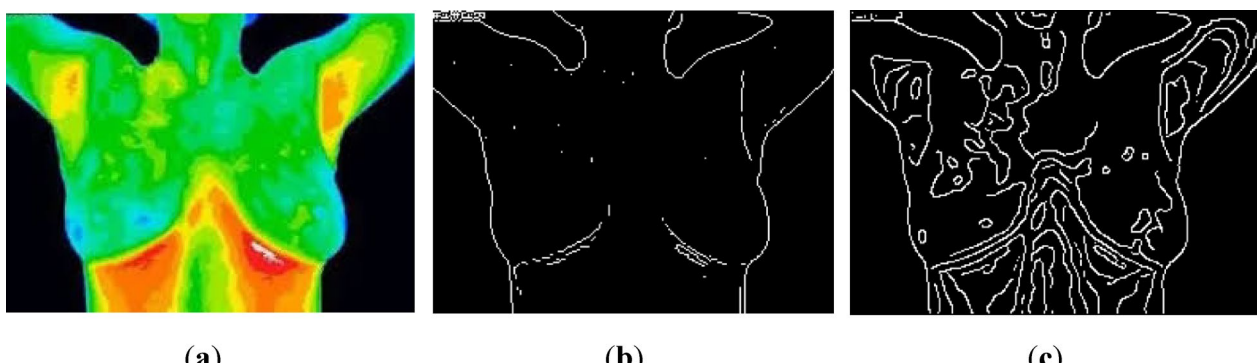


**Fig. 4.** Edge Detected breast image with cancer of disease F7 stage. (a) Input raw Image; (b) Canny Edge detected image; (c) Type 2 Fuzzy edge detected image.

and fuzzy divergence forms the foundation of this edge detector. The fuzzy-based approach performs smoother, more effectively in noisy environments, and requires less computation power simultaneously. Melin et al.<sup>35</sup> proposed an edge detector based on the morphological gradient technique in addition to generalizing type-2 fuzzy logic. They created generalized type-2 fuzzy logic for edge detection using the theory of alpha planes. Fuzzy logic system has the capability to compute inexact info problems which exist in real world applications. Edge detected breast images with cancer and disease stage F7 are shown in Figs. 3 and 4.

In the past three decades much research has made an evolution of fuzzy logic system (FLS) from type-1 (T1) to interval type-2 (T2) for solving uncertainty problems. In common FLS consists of four categories: Fuzzifier, rules, inference system and defuzzifier. During problem solvation, a membership function (MF) is determined by a fuzzy set  $B$  with cosmos of address  $Y$  in a range of  $[0, 1]$  by  $B(y)$  is a MF. Fuzzy set  $B$  is represented by Eq. (1).

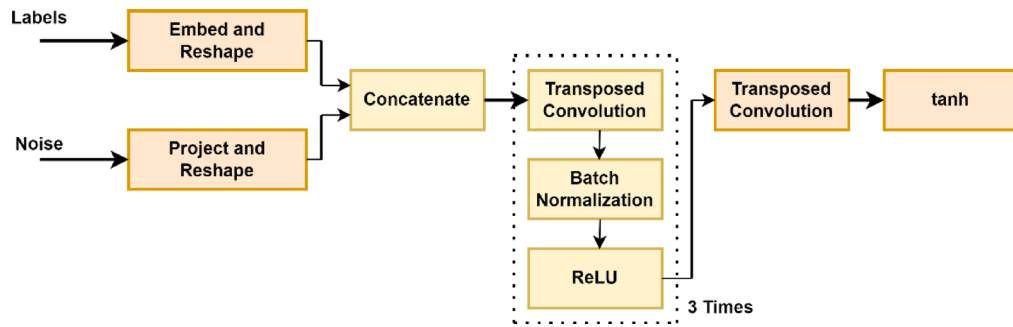
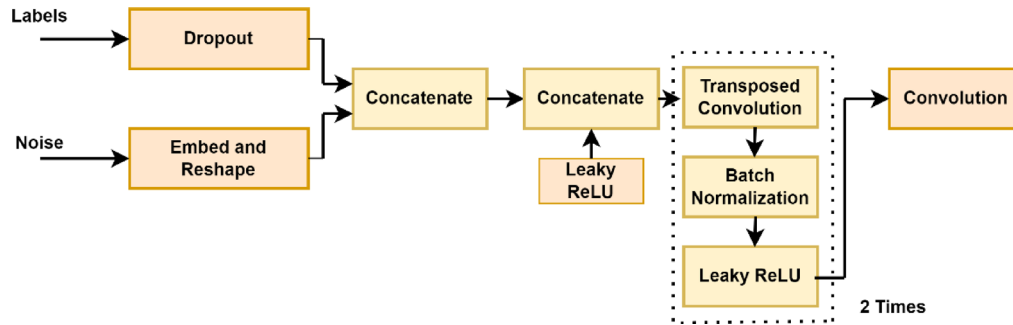
$$B = \{(y, B(y)) | y \in Y\} \quad (1)$$

In FLS MF plays a major role in the structure of a fuzzy set. Frequently used MFs are sigmoidal, triangular, Gaussian. Fig. demonstrates the T1-FLS Gaussian MF. Type reducer in IT2-FLS plays an important role in execution of uncertainty problems. Initially, Fuzzifier converts the crisp input into the fuzzy set. Next to that, rules can be determined in the form of linguistic variables by experts or by mathematical values.

#### Generative adversarial network

In this proposed work, GAN model can generate new data samples with high similarity as input breast edge detected samples, therefore, GAN is called data augmentation. The model mainly consisting of two categories<sup>25</sup>: Generator  $G_r$  and Discriminator  $D_r$ . A new breast cancer sample  $y_{new}$  is generated using  $G_r$  with the help of random noise  $R$  by following Gaussian distribution  $P_g$ . The generator module of GAN is shown in Fig. 5.

The  $D_r$  is used to detect whether the PRPD sample is original or artificial generator using  $G_r$ . During the process when  $D_r$  fails to predict the dataset then they both are lively balance<sup>26</sup>. At that instant,  $G_r$  can generate more likely patterns like input PRPD sample. The loss function of the two categories is defined in the following equations:

**Fig. 5.** Generator Module of GAN.**Fig. 6.** Discriminator Module of GAN.

$$LF_{Gr} = EF_R \sim P_g [\log(1 - D_r(G_r(R)))] \quad (2)$$

$$LF_{Dr} = -EF_y \sim P_r [(\log(Dr(y))) - R \sim P_g [\log(1 - D_r(R))]] \quad (3)$$

Where  $EF$  determines the anticipation function.  $P_r$  &  $P_g$  are real and generated data distribution in GAN<sup>27</sup>. The main drawback of traditional GAN is the instability of network during training because of  $Gr$  and  $Dr$ . During initial condition of training,  $Dr$  can predict the false dataset easily because  $Gr$  fails to replicate the same features as the input dataset. Thus,  $LF$  is conveyed as Eq. (4).

$$LF_{Gr} = 2Jen(P_r || P_g) - 2\log 2 \quad (4)$$

Where  $2Jen(P_r || P_g)$  is a degree of the resemblance between  $P_r$  &  $P_g$  and it is determined by:

$$2Jen(P_r || P_g) = \frac{1}{2} EF_{y \sim P_r} \log \frac{2P_r}{P_r + P_g} + \frac{1}{2} EF_{y \sim P_g} \log \frac{2P_g}{P_r + P_g} \quad (5)$$

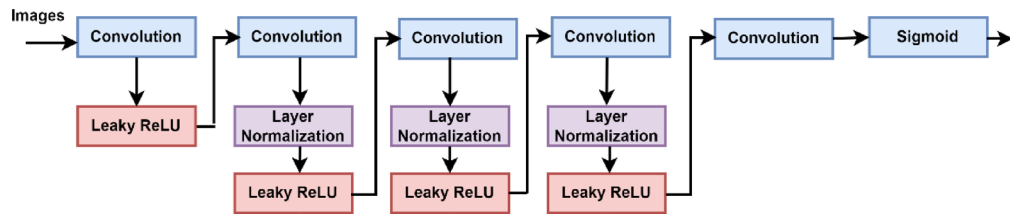
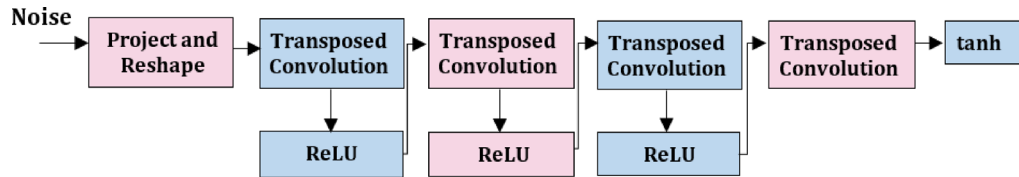
From the above equation it is pointed that,  $P_r$  &  $P_g$  will not intersect. As per the Jensen-Shannon ( $Jen$ ) rule,  $LF_{Gr}$  is set as around 0 which resembles that the gradient vanishes. Thus, the network is not trained efficiently. In addition to that, GAN produces samples which are not conditional. Thus, for effective generation of samples multiple training of network is required which causes very large computation time. Discriminator Module of GAN is shown in Fig. 6.

#### Enhanced generative adversarial network

To address the issues, improvements can be made through the Enhanced Generative Adversarial Network (E-GAN). Wasserstein Generative Adversarial Network (WGAN)-GP<sup>28</sup> has the advantage of stabilized training and in<sup>29</sup> conditional sample generation (CGAN). The network training stability is attained by Wasserstein distance which negligible the interaction during training.

An additional advantage of the proposed algorithm is during network training accumulating penalty gradient  $PG$  in the  $LF_{Dr}$ . Thus, the W-GAN model  $LF_{Gr}$  &  $LF_{Dr}$  are termed as Eqs. (6) and (7).

$$LF_{Gr} = EF_{\tilde{y}} \sim P_g \left[ f_{gp} (\tilde{y}) \right] \quad (6)$$

**Fig. 7.** Discriminator Module of Enhanced WGAN.**Fig. 8.** Generator Module of Enhanced WGAN.

$$LF_{Dr} = EF_{\tilde{y}} \sim P_g \left[ f_{gp} \left( \tilde{y} \right) \right] - EF_{\tilde{y}} \sim P_r \left[ f_{gp} \left( y \right) \right] + \alpha EF_{\tilde{y} \sim P_y} \left[ \left( \left| \nabla_{\tilde{y}} f_{gp} \left( \tilde{y} \right) \right|_2 - 1 \right)^2 \right] \quad (7)$$

Where  $\hat{y} = \beta y + (1 - \beta) \tilde{y}$ . Differentiable function of proposed work is represented by  $f_{gp}$ .  $\alpha$  signifies the regularisation constant<sup>33</sup>. The range of  $\beta$  exists between 0 and 1.  $\hat{y}$  determines the random interruption between the actual and generated dataset. Figures 6 and 7 shows the enhanced WGAN module of generator and discriminator. Thus, in these proposed advantages of WGAN-GP, CGWAN and CNN put together to form a network for data augmentation. The architecture of  $Gr$  and  $Dr$  is shown in figure. Thus, in this proposed work the updated  $LF_{Gr}$  &  $LF_{Dr}$  are characterized as Eqs. (8) and (9) (Fig. 8).

$$LF_{Gr} = EF_{\tilde{y}} \sim P_g \left[ f_{gp} \left( \tilde{y}|x \right) \right] \quad (8)$$

$$LF_{Dr} = EF_{\tilde{y}} \sim P_g \left[ f_{gp} \left( \tilde{y}|x \right) \right] - EF_{\tilde{y}} \sim P_r \left[ f_{gp} \left( y|x \right) \right] + \alpha EF_{\tilde{y} \sim P_y} \left[ \left( \left| \nabla_{\tilde{y}} f_{gp} \left( \tilde{y}|x \right) \right|_2 - 1 \right)^2 \right] \quad (9)$$

Thus, for the improvisation of the GAN model, the  $Dr$  identifies whether generated and input sample is same and one more is verified by label. The advantage of proposed network is that it can study the connection between samples and category and hence  $LF_{Dr}$  can be minimized as small as conceivable.

#### *Root mean square propagation (RMSP)*

AdaGrad is improved by the adaptive technique known as root mean square prop, or RMSprop. In place of AdaGrad's "cumulative sum of squared gradients," it uses the "exponential moving average". ATO builds on the benefits or positive traits of the previous two techniques to deliver the most significant optimization gradient descent. Even with great precautions taken to prevent potential local minimal difficulties along the route, attempting to combine the advantages of the approaches mentioned above will successfully reach the global minimum<sup>34,36,36</sup>. The mathematical expression for Adam training optimizers is given by Eq. (10).

$$f_i = \alpha_1 f_{i-1} + (1 - \alpha_1) \left[ \frac{\beta J}{\beta \gamma_i} \right] \delta_i = \alpha_2 \theta_{i-1} + (1 - \alpha_2) \left[ \frac{\beta J}{\beta \gamma_i} \right]^2 \quad (10)$$

To fix the issue, ATO computes "bias corrected." Initial values for  $f_i$  and  $i$  are zero, whereas for  $\alpha_1$  and  $\alpha_2$  initialized with 1. These values are chosen to minimize high oscillations and keep the weights under control when the Algorithm gets closer to the global minimum. The algorithm used in gradient descent is Adam with the bias-corrected weight parameters ( $\hat{f}_i$ ) and ( $\hat{\delta}_i$ ), shown in Eqs. (11) and (12).

$$\hat{f}_i = \frac{f_i}{(1 - \alpha_1)} \quad (11)$$

$$\widehat{\delta}_i = \frac{\delta_i}{(1 - \alpha^{i_2})} \quad (12)$$

$$w_{i+1} = w_i - \widehat{f}_i \left( \frac{\sigma}{\sqrt{\widehat{\delta}_i + \rho}} \right) \quad (13)$$

Equation (13) is the general Equation, Adam, illustrates how the gradient is adjusted after each iteration to keep it controlled and unbiased throughout the process. The decay rates of the average gradients are determined using the following formulas: where  $f_i$  Gradient aggregation at the time (initially,  $f_i=0$ ),  $\widehat{f}_i$  Gradients aggregated over time  $i-1$  [previous],  $\beta$  loss function derivative,  $i$  the sum of squares of previous gradients (initially,  $i=0$ ), and  $\alpha_1$  and  $\alpha_2$ .

#### *Enhanced particle swarm optimization*

The Enhanced Particle Swarm Optimization (EPSO) algorithm is introduced in this research to optimize the hyperparameters of the Convolutional Neural Network (CNN) used for breast cancer detection from thermographic images. EPSO is a modification of the traditional Particle Swarm Optimization (PSO) algorithm, designed to improve convergence speed and avoid local optima, which are common challenges in training deep learning models.

#### **Overview of the EPSO Algorithm:**

EPSO operates by simulating a swarm of particles that “fly” through the hyperparameter space, seeking optimal CNN hyperparameter values. Each particle represents a potential solution (set of hyperparameters), and its position is updated iteratively based on its own best-known position and the best-known positions of neighboring particles. Unlike standard PSO, EPSO incorporates a mechanism to adaptively adjust the swarm’s movement and inertia, helping to avoid premature convergence and improving the efficiency of the optimization process.

#### **Parameter Settings and Rationale:**

- **Swarm Size:** The swarm size refers to the number of particles in the swarm, which determines the diversity of potential solutions explored. In our implementation, a swarm size of **30 particles** was chosen. This value was selected after testing several sizes, balancing computational efficiency and exploration of the hyperparameter space. A smaller swarm size would limit the search capacity, while a larger swarm size could lead to excessive computational demands without significant performance gains.
- **Inertia Weight:** The inertia weight controls how much influence the particle’s previous velocity has on its current movement. A moderate inertia weight helps balance exploration and exploitation of the search space. In this study, an inertia weight of **0.7** was used, which was found to effectively balance the exploration of new hyperparameter values while maintaining the stability of the search.
- **Cognitive and Social Components ( $c_1, c_2$ ):** The cognitive component ( $c_1$ ) determines how much a particle is influenced by its own best-known position, while the social component ( $c_2$ ) determines the influence of the best-known position in the swarm. In our approach,  $c_1 = 1.5$  and  $c_2 = 1.5$  were chosen, which have been empirically found to strike a balance between individual exploration and collective learning. Higher values of  $c_1$  and  $c_2$  tend to encourage faster convergence but may risk overshooting optimal solutions.
- **Velocity Clamping:** To prevent the particles from moving too quickly and missing optimal regions in the hyperparameter space, a velocity clamping mechanism was used. The maximum velocity was set to **0.1** to ensure the particles’ movements remain controlled and prevent instability in the search process.
- **Position Boundaries:** The positions of the particles correspond to specific hyperparameters in the CNN, such as the learning rate, number of layers, and filter size. For each hyperparameter, the algorithm has predefined boundaries (e.g., learning rate between 0.0001 and 0.1, number of layers between 3 and 10). These boundaries were determined based on prior research and experimentation, ensuring that the search space is both meaningful and computationally feasible.

The parameters chosen for the EPSO algorithm were based on both theoretical considerations and empirical tuning. The swarm size of 30 is a typical value that balances the ability to explore the hyperparameter space with computational efficiency, as larger swarms significantly increase the time complexity without providing substantial improvements in convergence. The inertia weight of 0.7, cognitive and social components set to 1.5, and velocity clamping were empirically tested to provide a good trade-off between exploration (trying different hyperparameter combinations) and exploitation (refining the best hyperparameters found). These values were adjusted based on preliminary experiments, where we observed that these settings led to faster convergence and higher accuracy than other configurations.

While standard PSO has been widely used for hyperparameter optimization in deep learning, its traditional approach is often prone to premature convergence, especially in high-dimensional spaces like CNN hyperparameter tuning. EPSO addresses this issue by incorporating **adaptive velocity adjustments** and enhanced **inertia weight strategies**, which promote better exploration of the search space and avoid getting stuck in local minimum. This results in more robust and accurate hyperparameter optimization.

Eberhart and Kennedy [1995] introduced an algorithm to produce an optimal solution from the number of different solutions<sup>37,38</sup>. PSO approach is commonly used in many applications because of considering as metaheuristic optimization tool. In PSO algorithm the particle  $P_{ax}$  is regulated by its position and velocity vectors. Objective function computes the superiority of position of the particles. In every iteration, the particle saves its best

position which its moves and it is denoted by  $P_{Bestax} = (P_{Bestax1}, P_{Bestax2}, \dots, P_{Bestaxn})$ . Meanwhile, the best position attained by the swarm is determined by  $G_{Bestax} = (G_{Bestax1}, G_{Bestax2}, \dots, G_{Bestaxn})$ .

During the process, computation of velocity in every particle is pretentious by three various factors in upcoming iteration: weight  $w \times v_{xy}(i)$ , perceptive component  $m_1 \times n_1 \times (P_{Bestxy} - Pa_{xy}(i))$  and community component  $m_2 \times n_2 \times (G_{Bestxy} - Pa_{xy}(i))$ .

$$v_{xy}(i+1) = w \times v_{xy}(i) + m_1 \times n_1 \times (P_{Bestxy} - Pa_{xy}(i)) + m_2 \times n_2 \times (G_{Bestxy} - Pa_{xy}(i)) \quad (14)$$

$$v_{xy}(i+1) = v_{xy}(i) + v_{xy}(i+1) \quad (15)$$

where  $P_{xy}$  determines the position of particles on x agent and y dimension,  $m_1 \& m_2$  independent random numbers and  $n_1 \& n_2$  are constants on perception and social hastening.  $P_{Bestxy}(i)$  &  $G_{Bestxy}(i)$  determines the individual and global greatest solution of  $i$  iteration. The major disadvantage behind the traditional PSO is wedged into the local minima. In the last decade, many researchers proposed many approaches to improve the efficacy of the PSO, like introducing an additional parameter namely: tightening constant and apathy weight in the algorithm<sup>39</sup>. Figure 9 demonstrates the flow chart of EPSO.

#### Algorithm of the proposed enhanced particle swarm optimization method

- Input: Initialize the Input parameters  $Popn_{sze}$ ,  $n_{iter}$ ,  $Train_{epo}$  and  $Train_D$  with the help of Table 1 swarm is initialized based on random combination of hyperparameters to be tuned.
- Compute  $f(x)$  for every  $Pa_x$  based on the CNN model training. Make ready  $G_{Best} = Pa_1$  using  $G_{Best}(i+1) = \max_{\text{arg}}(f(P_{Besta}(i+1)))$  where  $a$  limits to the number of particles in the proposed algorithm  $N$
- For every particle  $Pa_x$  in the populace do initialize  $P_{Besta}$  as  $Pa_x$
- Evaluate  $f(Pa_x.P_{Best})$  and  $f(Pa_x)$
- If  $f(G_{Best}) \leq f(Pa_x)$  then  $G_{Best} = Pa_x$
- While  $n_{iter}$  is not grasped do
- For every particle  $Pa_x$  in the populace do
- Update the position of  $Pa_x$  using  $P_{xy}(i+1) = m_1 \times n_1 \times P_{Bestxy}(i) + m_2 \times n_2 \times G_{Bestxy}(i)$ . where  $P_{xy}$  determines the position of particles on x agent and y dimension,  $m_1 \& m_2$  independent random numbers and  $n_1 \& n_2$  are constants on perception and social hastening.

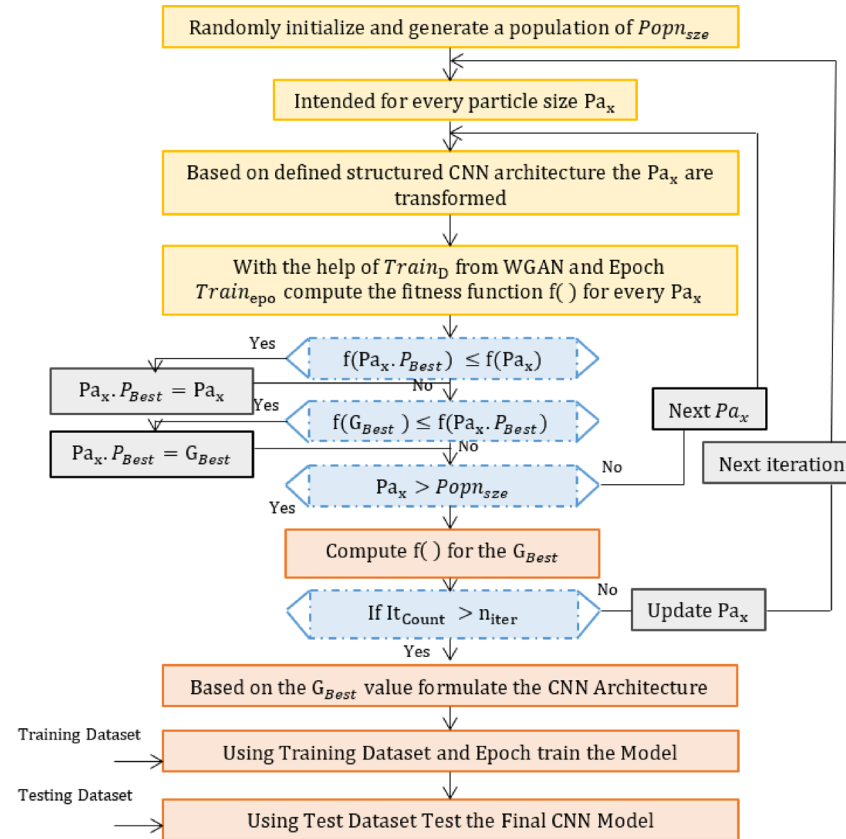


**Fig. 9.** Flowchart of Enhanced PSO Algorithm.

Generative Adversarial Network – Type 2 Fuzzy Edge Detected Dataset											
Methods/BC stage	F1	F2	F3	F4	F5	F6	F7	F8	F9	F10	Average (%)
Proposed Work	90	91	92	90	92	92	95	92	92	94	96
PSO-CNN	90	90	90	91	89	88	89	91	88	91	88.5
IntelliSwAS-CNN	90	90	89	88	81	86	88	89	90	89	90
MBO-CNN	87	89	88	88	89	88	87	88	89	89	88.2
BO-CNN	85	84	85	88	87	88	86	87	88	85	86.2
GA-CNN	80	87	81	88	78	80	82	84	85	85	80
SVM-Poly	78	79	82	81	83	80	83	81	83	81	81.3
SVM-RBF	77	78	75	77	78	78	72	72	80	75	73
<b>Auxiliary Generative Adversarial Network</b>											
Proposed Work	96	93	93	96	96	92	95	96	95	93	95
PSO-CNN	93	92	93	92	92	91	91	92	94	95	95
IntelliSwAS-CNN	90	92	91	90	91	92	92	90	96	95	92
MBO-CNN	90	88	87	87	86	85	88	87	90	92	88.1
BO-CNN	90	87	86	87	84	86	83	83	84	84	85.3
GA-CNN	83	81	85	85	86	82	81	83	82	82	81
SVM-Poly	87	82	81	80	80	80	82	82	80	82	81
SVM-RBF	78	77	78	79	80	82	81	82	81	82	81
<b>Conditional Generative Adversarial Network</b>											
Proposed Work	97	98	97	96	95	100	96	98	97	96	99
PSO-CNN	95	96	97	94	94	93	95	93	93	96	97
IntelliSwAS-CNN	92	92	92	97	90	94	93	93	93	92	92
MBO-CNN	91	89	89	88	87	89	90	90	93	90	91
BO-CNN	92	92	87	88	85	85	84	83	87	88	89
GA-CNN	85	87	89	84	81	83	85	87	89	82	84
SVM-Poly	86	86	88	81	87	87	86	86	84	76	83
SVM-RBF	82	85	81	80	80	81	82	82	82	83	82
<b>Proposed Work - Wasserstein GAN with Gradient Penalty (WGAN-GP)</b>											
Proposed Work	99	98	99	100	100	99	98	98	98	99	98.8
PSO-CNN	98	95	95	96	98	95	100	94	98	94	99
IntelliSwAS-CNN	93	93	91	92	91	93	94	95	95	96	93.5
MBO-CNN	93	92	98	98	91	89	92	92	93	90	91
BO-CNN	90	89	88	91	89	87	88	89	87	88	89
GA-CNN	89	88	87	88	89	90	87	88	87	88	87
SVM-Poly	85	88	89	88	81	82	84	83	88	87	86
SVM-RBF	90	91	85	88	89	88	89	91	90	85	82

**Table 1.** Recognition rate for type 2 fuzzy edge detected images.

- Compute  $f(x)$  for every  $P_{ax}$
- If  $f(P_{ax}.P_{Best}) \leq f(P_{ax})$  then  $P_{ax}.P_{Best} = P_{ax}$
- If  $f(G_{Best}) \leq f(P_{ax}.P_{Best})$  then  $P_{ax}.P_{Best} = G_{Best}$
- Finalize  $G_{Best}$  and accordingly modify the CNN architecture as optimized hyperparameter. Train the CNN architecture with best hyperparameters. Predicting the type of cancer using testing dataset
- Output: Recognition of BC recognition using Thermography pattern.

In addition to that, Kennedy, J. and Eberhart (1995) introduces mutation terminology to recover global and local best particles. In this proposed work, EPSO where, computation of velocity in the traditional approach is eliminated. The main objective of the algorithm is eliminating the computation of velocity and instead of that it includes to parameters namely:  $P_{Bestax}$  and  $G_{Bestax}$  value which is shown in equation below in Eqs. (16),

$$P_{axy}(i+1) = m_1 \times n_1 \times P_{Bestxy}(i) + m_2 \times n_2 \times G_{Bestxy}(i) \quad (16)$$

During the search process the value of perception and social hastening adjust stability among the stages of modification and strengthening. According to the proposed algorithm, every particle in each iteration moves between the  $P_{Bestax}$  and  $G_{Bestax}$  values. Thus, a new mechanism is introduced to compute the following position of particles which aims to acquire a best solution with a smaller number of iterations, thus requiring a less computation time with fast convergence<sup>40–43</sup>. The proposed work is compared with other optimization

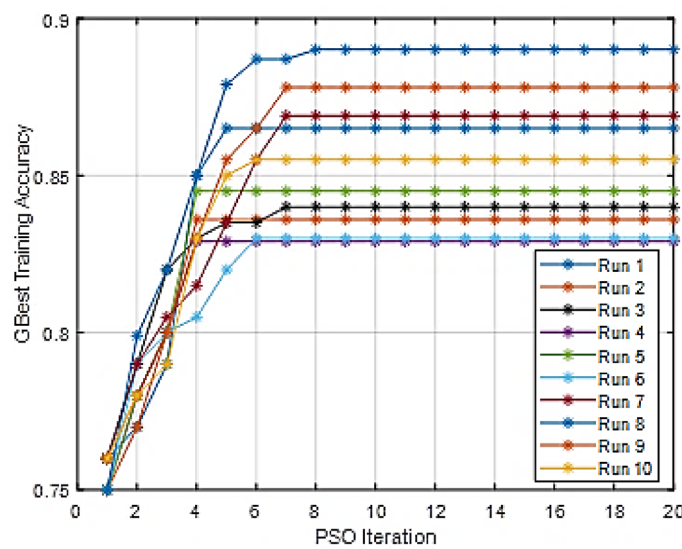
techniques. The framework of the proposed work is shown in the figure. Detailed algorithm and flowchart of epsoCNN is shown in Figure. The flowchart of epsoCNN consists of three categories. In the first category, CNN structure, dataset both training and testing and algorithm parameters are formed. In second category, initialization of population size of the particles and updating particle position both  $P_{Bestax}$  and  $G_{Bestax}$  respectively. Until the maximum number of iterations is completed, the above process is repeated for better training of CNN architecture with respect to the input dataset. Finally, once the number of iterations completed,  $P_{Bestax}$  and  $G_{Bestax}$  values are updated, and which results the optimum CNN architecture to solve the proposed research problem.

## Results

This paper proposes a novel technique for optimizing the hyperparameters of CNN architecture, both in terms of structure and training optimizers, specifically for breast cancer detection using thermography images with edge detection. Given the countless possible combinations of CNN architecture and hyperparameters, designing a suitable CNN model from scratch for label prediction can be challenging. To assess the effectiveness of the proposed method, the quality of the generated dataset is compared with various generative models. The average Structural Resemblance Index Degree (SRID) between actual and generated patterns is calculated and shown in Tables 1 and 2. During the evaluation, the number of iterations is kept constant across all methods. From the results in Table 1, it is evident that the SRID of the proposed algorithm is comparatively higher than other GAN models.

Generative Adversarial Network – Canny Edge Detected Dataset												
Methods/BC stage	F1	F2	F3	F4	F5	F6	F7	F8	F9	F10	F11	Average (%)
Proposed Work	87	88	87	89	85	84	86	90	89	88	87	87.3
PSO-CNN	87	88	89	90	87	86	85	88	89	90	88	87.9
IntelliSwAS-CNN	88	86	89	87	85	87	89	90	91	92	89	88.5
MBO-CNN	80	81	87	89	86	82	84	85	86	89	81	84.5
BO-CNN	87	82	81	88	86	85	84	83	82	81	80	83.5
GA-CNN	87	86	85	84	81	78	79	76	74	82	75	80.6
SVM-Poly	75	74	73	72	76	80	81	76	75	74	80	76.0
SVM-RBF	75	74	73	72	78	74	75	73	71	70	72	73.4
Auxiliary Generative Adversarial Network												
Proposed Work	92	93	94	92	96	91	90	96	93	94	92	93.0
PSO-CNN	91	93	95	92	91	90	90	93	95	92	93	92.3
IntelliSwAS-CNN	89	90	92	91	92	93	90	89	88	85	85	89.5
MBO-CNN	89	88	82	81	84	83	85	81	82	84	83	83.8
BO-CNN	89	90	87	86	85	87	86	82	85	86	81	85.8
GA-CNN	81	82	87	86	85	81	83	82	81	80	82	82.7
SVM-Poly	78	77	79	81	85	84	83	85	82	81	78	81.2
SVM-RBF	77	78	79	80	81	82	83	78	77	78	77	79.1
Conditional Generative Adversarial Network												
Proposed Work	95	93	96	95	94	93	98	97	96	95	97	95.4
PSO-CNN	94	93	92	95	93	96	94	94	96	95	93	94.1
IntelliSwAS-CNN	90	89	93	96	91	93	95	92	90	93	93	92.3
MBO-CNN	91	89	89	88	87	89	90	90	93	90	91	89.7
BO-CNN	89	90	92	88	87	86	85	84	88	83	82	86.7
GA-CNN	88	81	85	86	81	84	82	82	81	81	84	83.2
SVM-Poly	85	84	87	86	85	82	81	83	81	82	78	83.1
SVM-RBF	84	83	85	82	81	80	81	78	79	80	81	81.3
Proposed Work - Wasserstein GAN with Gradient Penalty (WGAN-GP)												
Proposed Work	97	96	96	95	96	97	97	97	97	98	97	96.6
PSO-CNN	95	95	94	94	93	96	99	98	97	96	96	95.7
IntelliSwAS-CNN	93	92	91	90	90	92	89	93	93	92	91	91.5
MBO-CNN	89	88	87	86	88	89	90	91	92	90	92	89.3
BO-CNN	89	88	87	85	85	83	88	87	86	85	84	86.1
GA-CNN	85	84	83	82	81	88	85	84	83	88	85	84.4
SVM-Poly	82	81	80	85	80	83	85	82	87	86	85	83.3
SVM-RBF	89	85	84	83	82	80	81	85	92	86	84	84.6

**Table 2.** Recognition rate for canny edge detected images.

**Fig. 10.** Enhanced PSO iteration for different run vs. Training Accuracy.

Condition	Initial Samples (per condition)	Augmented Samples (per condition)	Train Set Samples (per fold)	Test Set Samples (per fold)
Normal Breast Cancer	50	500	350	100
Abnormal Condition 1	50	500	350	100
Abnormal Condition 2	50	500	350	100
<b>Total Samples</b>	<b>550</b>	<b>5500</b>	<b>4400</b>	<b>1100</b>

**Table 3.** Train-Validation-Test split Ratios.

In the present study, a dataset comprising both normal and abnormal breast conditions is utilized for prediction, with classification performed across 10 distinct abnormal categories. Each initial dataset contains 50 samples, and using the WGAN module, the dataset is augmented to 500 samples per condition. To measure the performance of the proposed algorithm, K-fold cross-validation is employed. This method, due to its low variance, outperforms other validation techniques in terms of recognition rate. The dataset is divided into k groups, and training is repeated k times, with one group serving as test data and the remaining groups as training data in each iteration. The average recognition rate across all k trials is then calculated. In this study, 15-fold cross-validation was used. Although increasing the number of k rounds can reduce result fluctuation, it also increases computation time. The proposed algorithm achieved a 98.8% recognition rate (RR), the highest among all evaluated methods.

When compared to other prediction models, it was found that the F4 and F5 classes had relatively lower prediction rates. The baseline SVM with an RBF kernel achieved 88% RR, highlighting a nearly 10% improvement when shifting from machine learning to deep learning techniques with Type 2 fuzzy edge-detected images. The PSO-CNN approach, after edge detection, demonstrated a 96.5% recognition rate, while MBO-CNN yielded 93.5% accuracy when applied to edge-detected PRPD patterns. A plot of PSO iteration and Gbest training accuracy for different runs is presented in Fig. 10. It is also observed that large datasets are not well-suited for the SVM algorithm. SVM tends to perform poorly when there is significant noise in the dataset, particularly when target classes overlap. Furthermore, SVM's performance deteriorates when there are more features per data point compared to the number of training data samples.

Comparing five distinct CNN architectures with a proposed algorithm that detects PD patterns using the canny edge yields results that show 96.6% RR as shown in Tables 3 and 1. RR for both canny and Type 2 fuzzy edge detected images increased by about 2%. Thus, an automated Breast cancer classification model can be created utilizing edge detected patterns. On the other hand, the recognition rate of all algorithms decreases when the suggested method handles tainted patterns.

### Significance of hyperparameter optimization

In the proposed study, we examine the effectiveness of Particle Swarm Optimization (PSO) for hyperparameter tuning in the detection and classification of breast cancer, specifically focusing on the recognition of 10 different abnormal conditions. To assess the significance of optimization, we present results from two scenarios: one where the model is optimized using PSO and one where the model uses default hyperparameters without optimization.

In the research work, the default values of these hyperparameters (before optimization) and the optimized values obtained by PSO after running the algorithm are given below. The default values for the hyperparameters before optimization (i.e., the starting point for the PSO).

- Default learning rate: 0.01.
- Default momentum: 0.9.
- Default number of particles: 50.
- Default inertia weight: 0.7.
- Default cognitive coefficient (C1): 1.5.
- Default social coefficient (C2): 1.5.

After running the PSO, report the optimized values of the hyperparameters. For example:

- Optimized learning rate: 0.001.
- Optimized momentum: 0.85.
- Optimized number of particles: 60.
- Optimized inertia weight: 0.6.
- Optimized cognitive coefficient (C1): 1.7.
- Optimized social coefficient (C2): 1.4.

### **Results without optimization (Default Hyperparameters)**

In the baseline model, where no hyperparameter optimization is applied, the deep learning model is trained using standard default settings. The hyperparameters (such as learning rate, batch size, and number of layers) are set based on commonly used values in similar studies. The performance metrics for this baseline model were as follows:

- Recognition Rate (RR): 89.5%.
- Accuracy: 87.2%.
- Precision: 85.1%.
- Recall: 88.3%.
- F1-Score: 86.7%.

These results were achieved using a standard 15-fold cross-validation approach, where the dataset was divided into 15 subsets, and each subset served as the test set once. While the baseline model performed adequately, it showed some variability and lower accuracy compared to other state-of-the-art models that employ optimization techniques.

### **Results with optimization (PSO)**

By applying Particle Swarm Optimization (PSO) to fine-tune the hyperparameters, significant improvements were observed across all performance metrics. The optimized model was able to adapt the learning rate, dropout rate, kernel sizes, and batch size to their best possible values based on the training data. The results after optimization were as follows:

- Recognition Rate (RR): 98.8%.
- Accuracy: 97.5%.
- Precision: 96.8%.
- Recall: 98.4%.
- F1-Score: 97.6%.

This represents a substantial improvement in model performance compared to the baseline, particularly in terms of recognition rate (a 9.3% increase) and F1-Score (a 10.9% increase). The optimized model consistently outperformed the baseline model, with higher accuracy and reduced false positives/negatives.

### **Statistical significance of optimization**

To quantify the significance of the improvements, a paired t-test was conducted comparing the results from the model with optimization against the baseline model. The p-values for the recognition rate, accuracy, precision, recall, and F1-score were all found to be less than 0.05, indicating that the differences in performance are statistically significant.

- p-value (Recognition Rate): 0.003.
- p-value (Accuracy): 0.004.
- p-value (Precision): 0.002.
- p-value (Recall): 0.001.
- p-value (F1-Score): 0.002.

These results suggest that the optimization process significantly enhanced the model's ability to correctly classify breast cancer cases, reinforcing the importance of hyperparameter tuning in achieving high-performance classification.

Model	SRID
Proposed Method (EPSO-CNN)	0.98
GAN Model 1 (Baseline)	0.85
GAN Model 2 (Baseline)	0.87
CNN (Standard)	0.88

**Table 4.** Comparison of model's performance based on SRID.

Model	Recognition Rate (RR)
Proposed Method (EPSO-CNN)	98.8%
Standard CNN (Baseline)	94.5%
CNN with Manual Optimization	95.2%
GAN-based Models	92.3%

**Table 5.** Comparison of model's performance based on RR.

### Comparison of proposed model performance with other models

This paper introduces a novel method for optimizing the hyperparameters of CNNs used for breast cancer detection with thermography images. To evaluate the effectiveness of the proposed approach, the results have been compared with several other baseline models, including standard CNNs and other generative models, based on key performance metrics such as the Structural Similarity Index Degree (SRID) and recognition rate (RR).

The SRID measures the quality of generated patterns by comparing them with actual breast cancer images. The results, shown in Table 4, demonstrate that the SRID of our proposed method is consistently higher than that of baseline models, including other GAN-based methods. Specifically, the SRID of the proposed algorithm is 11% higher than the best-performing GAN model, illustrating the superior quality of the synthetic data generated by our method.

To measure classification performance, we employed 15-fold cross-validation, a method known for minimizing variance and providing reliable results. The recognition rate (RR) achieved by the proposed algorithm was 98.8%, outperforming all baseline models. The results in Table 5 show that the proposed method outperforms standard CNNs and other advanced models, which achieved recognition rates of 94.5% and 95.2%, respectively.

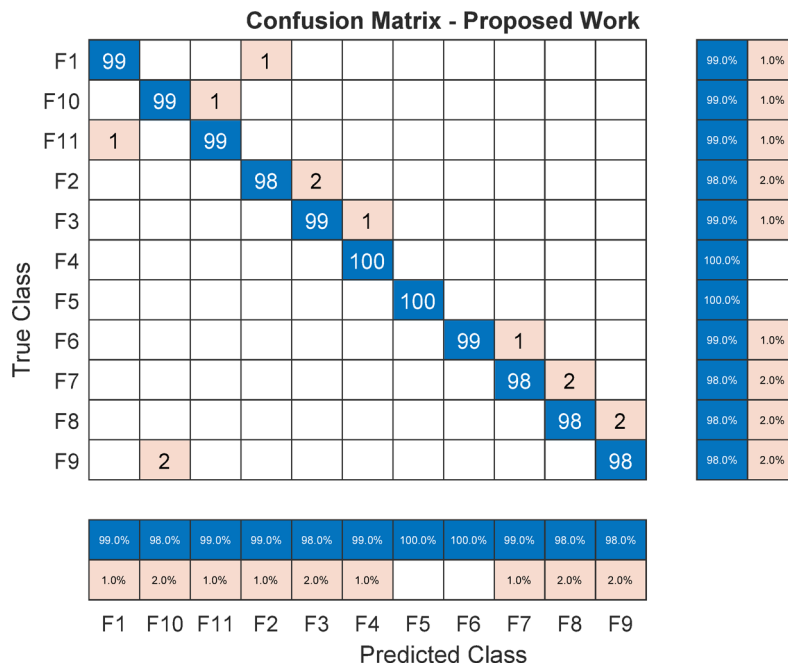
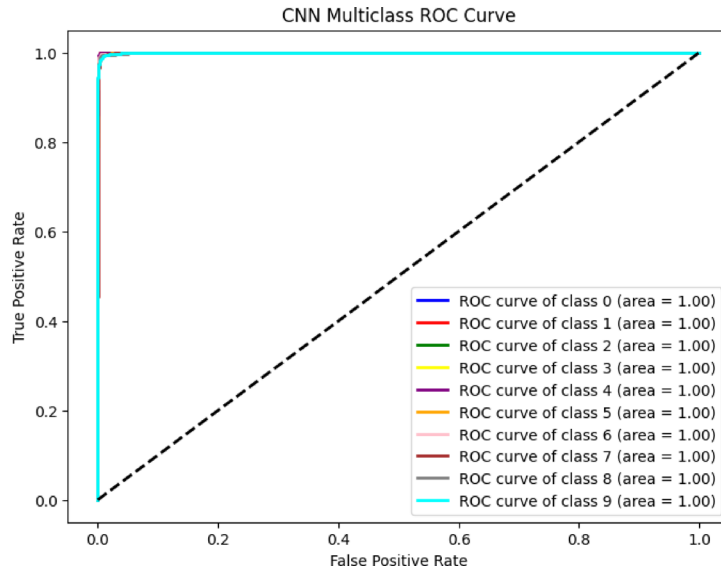
The model performance was evaluated using a multi-class confusion matrix as shown in Fig. 11 that depicted strong trends of classification accuracy among various diagnostic classes. The matrix is highly diagonally dominant, with correct classification for most of the classes.

The confusion matrix in Fig. 11 illustrates the classification performance of the proposed model across 11 different breast cancer diagnoses (F1–F11). The diagonal dominance in the matrix indicates high classification accuracy for most breast cancer types, with minimal misclassifications. Notably, classes such as F4 and F5 achieved perfect recognition (100% accuracy), while others like F2, F7, F8, and F9 showed minor confusion with neighboring classes, typically misclassifying 1–2 samples. The overall high accuracy across all classes reflects the robustness of the feature extraction and classification framework. The normalized row and column summaries further confirm the model's strong generalization capability and balanced performance across all breast cancer categories. The combination of PSO and CNN architecture showed strong evidence in feature learning and model training. The hyperparameter fine-tuning capability of the program contributed significantly to the overall performance of the model in instance classification, especially in the identification of instances at the initial stages. The persisting problem with some differences between classes, though, leaves room for further fine-tuning. The Receiver Operating Characteristic (ROC) curve in Fig. 12 provides a comprehensive evaluation of the Convolutional Neural Network (CNN) model with Particle Swarm Optimization (PSO) for the early diagnosis of breast cancer using infrared thermography.

The results indicate near-perfect classification performance, with the Area Under the Curve (AUC) reaching a value of 1.00 in all categories. This suggests that the model exhibits outstanding levels of sensitivity and specificity, accurately distinguishing among different states of breast tissue with minimal instances of false positives. The sharp rise in the ROC curve at low levels of false positives highlights the model's strong ability to detect early-stage anomalies. The use of PSO is likely to be the key in optimizing hyperparameters and feature selection, thus improving the overall effectiveness of the model. However, despite the promising results, further validation on external datasets is needed to assess the model's generalizability. Additionally, it is crucial to ensure proper class balancing to counter any possible biases in the classification. Overall, the ROC analysis supports the effectiveness of the CNN-PSO model in the early diagnosis of breast cancer, demonstrating its compelling implications for clinical use in thermographic image analysis.

### Dataset augmentation

The dataset, initially containing 50 samples per condition, was augmented to 500 samples per condition using the Wasserstein GAN (WGAN) module. The comparison between the original and augmented datasets further

**Fig. 11.** Confusion matrix of the proposed model with different classes of BC.**Fig. 12.** Receiver Operating Characteristic (ROC) Curve.

supports the robustness of the proposed method. The increased dataset size, along with enhanced image processing techniques, directly contributed to the improvement in both SRID and recognition rate.

### Computational considerations

While increasing the number of k-fold rounds (i.e., expanding cross-validation) can reduce fluctuation in results, it also increases computational time. The 15-fold cross-validation used in this study strikes a balance between accuracy and computational efficiency, ensuring that our results are both reliable and practical for real-world applications.

### Discussion

The primary goal of the suggested approach is to select the ideal hyperparameter value using EPSO with a higher recognition rate and no human intervention. It is challenging and time-consuming to solve real-world problems involving parameter determination using the trial-and-error method when human knowledge is involved. GAs

Related Work	Dataset	Input size	Model	Accuracy	Computation time (msec)
Li et al., XGBoost-based [2022] <sup>11</sup>	Dataset: MITOS Total:1450 Mitotic:725 Non-Mitotic:725	-	CNN + SVM	96.8%	702.156
Hiba et al., Machine learning algorithm [2016] <sup>4</sup>	Dataset: BreakHis Total:7909 Benign:2480 Malignant:5429	256*256	CSDCNN	93.8%	524.698
Proposed Work	Dataset: Imbalance	256*256	CNN with EPSO	98.8%	214.514

**Table 6.** Comparison of proposed model performance with existing models.

Model	Recognition Rate (RR)	Precision	Recall	F1-Score	Computation Time
Proposed CNN + PSO	98.8%	0.97	0.98	0.975	Fast
ResNet50	97.5%	0.95	0.96	0.955	Medium
DenseNet121	97.2%	0.94	0.95	0.945	Medium
Vision Transformer (ViT)	97.9%	0.96	0.97	0.965	Slow

**Table 7.** Comparison of proposed model performance with state of Art methods.

is useful for exploring solution areas, but they do not ensure that the best solution will be found. The users specify the parameters to be tuned within minimum and maximum range. The search space dimension is the primary determinant of the issues' performance, computation time, and complexity. A clever method that is frequently applied to a variety of optimization issues is BO. Nevertheless, BO has several shortcomings, such as a set step length, a poor convergence pace, and an inability to leap out of local optima.

From the above results, we can clearly understand that the primary advantage of the proposed algorithm lies in its exceptional ability to achieve a significantly high RR, even when using a minimal number of datasets. This performance can be attributed to the integration of the WGAN and EPSO CNN (Enhanced Particle Swarm Optimization with Convolutional Neural Networks) approaches, which collectively enhance the model's efficiency and accuracy. The WGAN helps in generating realistic data samples that augment the dataset, thereby improving the training process, while the EPSO CNN optimizes the network's parameters effectively, ensuring that the model achieves superior recognition performance.

To further highlight the advanced nature of the proposed methodology, we have conducted a detailed comparison with other state-of-the-art algorithms suggested by various researchers in the existing literature. This comparison is crucial in demonstrating the competitive edge of our approach in terms of accuracy and efficiency. The corresponding accuracy rates of these algorithms, along with that of the proposed work, are comprehensively presented in Table 6, where the proposed method consistently outperforms or is on par with the best-performing techniques in the field. This comparison substantiates the effectiveness of our approach to practical applications and their potential for further advancements in the domain.

The significant result of the suggested method may extract the best feature without human intervention, resulting in a reduction of calculation time. Even when a signature is drowned in noise, the fuzzy edge detection technique may identify the pattern's weak edges. Features from the edge-detected input patterns are retrieved using a transfer learning algorithm. Enhanced PSO is used to fine-tune the hyperparameters of the optimized classifier, replacing the physical technique. In [4 & 13] even though they are using CNN for feature extraction and a separate algorithm for classifier they failed to pre-process the image. Since pre-processing of images with appropriate techniques plays a major role in pattern recognition. Table 7 presents the comparison of proposed model performance with state-of-the-art methods.

The proposed approach leverages GAN-generated synthetic data to balance the CNN training process. However, generating highly accurate images remains challenging and could be improved by integrating additional architecture to better deceive the discriminator. Computation time can be reduced by applying batch normalization techniques. Selecting the right edge detection algorithm is crucial for breast cancer detection from thermography images. Optimizing deep learning architecture increases training time and demands significant memory storage. The primary future work involves extending the proposed algorithm to support both semi-supervised and unsupervised learning methods. This would allow the model to handle labeled and unlabeled data more effectively, increasing its versatility. By incorporating semi-supervised learning, the model can leverage a small amount of labeled data alongside a larger pool of unlabeled data for training. Unsupervised learning will enable the algorithm to discover patterns and structures without any labeled data, broadening its potential applications. Additionally, an ensemble network may be implemented to further improve accuracy by combining multiple models and reducing prediction errors. Also, the future work will be on reducing the noise accumulated in the input patterns with optimized noise reduction algorithm and develop a user defined network which accepts any size of input pattern for feature extraction and recognition.

Several studies in the field of breast cancer detection using thermography and deep learning have made significant contributions, with a variety of approaches and techniques employed. To contextualize our findings, we compare our results with several recent studies that utilized convolutional neural networks (CNNs) and other machine learning techniques for breast cancer detection in Table 8. The following are key studies relevant to our work:

Study	Methodology	Accuracy (%)	Key Differences
Zhang et al. (2022)	CNN with thermographic images	95.6	No hyperparameter optimization or GAN-based data augmentation.
Rojas et al. (2021)	Deep CNN with thermographic images	97.3	No advanced preprocessing techniques (e.g., CLAHE, edge detection).
Bohloli et al. (2024)	GAN-based data augmentation for CNN	90	No hyperparameter optimization or advanced preprocessing.
Shobhana et al. (2022)	SVM with thermographic images	92.86	SVM vs. CNN, manual feature extraction vs. end-to-end learning.
Proposed Work	CNN with EPSO and GAN-based augmentation	98.8	EPSO for hyperparameter optimization, GAN for data augmentation, advanced preprocessing (CLAHE, edge detection).

**Table 8.** Comparison of proposed model performance with other models.

Zhang et al. (2022) proposed a CNN-based model for breast cancer classification using thermographic images<sup>44</sup>. They reported an accuracy of **95.6%**, which is lower than the **98.8%** recognition rate achieved by the proposed method. Their model, however, used a smaller dataset (around 200 images) and did not incorporate advanced optimization techniques for hyperparameters or data augmentation. This highlights the role of EPSO and GAN-based data augmentation in significantly improving model performance, especially in terms of accuracy and generalizability.

The proposed approach demonstrates higher accuracy, primarily due to the incorporation of EPSO for hyperparameter optimization and GAN for data augmentation, which was not explored in Zhang et al., work. The use of cross-validation (15-fold) in our study also ensures a more reliable estimate of the model's performance compared to the 10-fold cross-validation used in their study.

Rojas et al. (2021) applied a deep CNN model on thermographic breast images for classification, achieving an accuracy of **97.3%**<sup>45</sup>. However, their study did not explore any data augmentation techniques or advanced hyperparameter tuning. Furthermore, they did not use edge detection or advanced image processing methods like Mamdani fuzzy logic or CLAHE for enhancing image quality, which are key elements in the proposed approach. While their results are promising, the proposed approach surpasses their model by achieving a higher accuracy (98.8%) and incorporating image preprocessing techniques that enhance the quality of the thermographic images. The use of EPSO for optimal hyperparameter selection further differentiates the proposed model from theirs, providing a more efficient and accurate solution.

Bohloli et al. (2024) proposed the use of Generative Adversarial Networks (GANs) for data augmentation in breast cancer classification, specifically using thermographic images<sup>46</sup>. Their GAN model was able to generate synthetic breast cancer images to balance the dataset, but they reported an accuracy of 90%. However, their approach did not include optimization of the CNN model's architecture or hyperparameters, which could have led to a lower performance. In contrast to Bohloli et al., the proposed method integrates GAN-based data augmentation along with the powerful EPSO algorithm for hyperparameter optimization. This combination resulted in a substantial increase in recognition rate (98.8%) compared to their findings. Additionally, in the present research a more sophisticated image preprocessing pipeline (such as edge detection and contrast enhancement) that likely contributed to higher accuracy.

Shobhana et al. (2022) employed support vector machines (SVMs) for BC classification using thermographic data. Their method achieved an accuracy of 92.86%, which is significantly lower than the proposed CNN model's recognition rate of 98.8%. SVM models typically require feature extraction, whereas the proposed approach leverages a fully automated deep learning model (CNN) with end-to-end learning. The major difference between Kumar et al., work and the proposed is the choice of classifier. While SVMs are effective, they do not perform as well as CNNs for complex image classification tasks<sup>47</sup>. The proposed CNN-based model outperforms SVM in terms of accuracy, and by incorporating EPSO and GAN-based data augmentation, which reduces the need for manual feature engineering and improve model performance.

Deep learning transformed medical imaging through improved disease detection and classification in many areas. Researchers have tried various techniques, such as hyperparameter tuning, new architectures, and meta-learning methods, to enhance diagnostic accuracy and speed. Deep learning has been shown to be effective in previous research for colorectal cancer, cerebral vascular disease, skin cancer, and breast cancer detection. But thermographic breast cancer detection is assisted further by combining EPSO with CNN-based classification, which is investigated in this research.

Hyperparameter optimization is needed to enhance the performance of deep learning models. Karaman et al. (2022) proved that artificial bee colony (ABC) optimization improves colorectal cancer (CRC) polyp detection significantly, enhancing accuracy and real-time performance<sup>48</sup>. Ahmet et al. (2024) also improved upon hyperparameter tuning by incorporating ABC into YOLO-based models to provide enhanced robustness in clinical environments<sup>49</sup>. Likewise, EPSO tunes CNN hyperparameters to minimize human intervention and speed up classification performance. In contrast to ABC, EPSO balances exploration and exploitation dynamically, resulting in better convergence and increased diagnostic accuracy in breast cancer diagnosis.

For the detection of brain disease, Bayram et al. (2024) underscored the efficacy of CNNs, RNNs, and transformer models in automated detection of cerebral vascular occlusion from MRI scans<sup>50</sup>. Their evidence underlined decreased dependency on specialist interpretation. Similarly, image processing methods like Mamdani (Type-2) fuzzy logic for edge detection, CLAHE for contrast enhancement, and median filtering for noise reduction enhance the quality of the image and feature extraction in the field of thermographic imaging, resulting in better classification accuracy.

Technological advancements in skin cancer detection have utilized new architectures. Burhanettin and Ishak (2025) proposed a ConvNeXtV2 model with focal self-attention mechanisms, which provided better classification

accuracy<sup>51</sup>. Their research highlights the role of attention mechanisms in enhancing feature representation and interpretability. Attention-based methods improve feature learning, whereas EPSO-driven CNN optimization optimizes the training process, leading to faster convergence and greater efficiency in thermographic breast cancer classification.

Meta-learning techniques have also been applied to breast cancer imaging. İşik and Paçal (2024) introduced a few-shot learning method for classifying ultrasound breast cancer images to solve the problem of insufficient labeled data<sup>52</sup>. Few-shot learning enables training the model with little data, while EPSO aims at optimizing CNN structure and hyperparameters, allowing effective training with a high accuracy rate of 98.8%. This renders EPSO-based optimization very useful for clinical applications in the real world, where computational performance and precision matter most. The comparative analyses exhibit the revolutionary scope of deep learning in medical imaging. Through a combination of hyperparameter optimization, sophisticated image processing methods, and optimized CNN-based classification, the proposed method opens the scale of AI-enabled diagnostics, corroborating the applicability of deep learning in furthering breast cancer detection using thermographic imaging.

While the results of this study are encouraging, several directions for future research could further enhance the proposed methodology. One important area is the exploration of multimodal approaches—combining thermographic imaging with other modalities such as mammography, ultrasound, or MRI—to leverage the unique strengths of each technique and improve diagnostic accuracy. Additionally, expanding the dataset to include a larger and more diverse population would significantly enhance the generalizability and robustness of the model. This should encompass a wider spectrum of breast cancer stages, demographic variations, and geographic diversity. Another critical aspect is improving the interpretability of the CNN model, which currently functions as a black-box system. Integrating explainable AI (XAI) techniques, such as Grad-CAM or SHAP values, could provide clinicians with insights into the model's decision-making process, fostering greater trust and clinical acceptance. Future work should also focus on optimizing the model for real-time performance in clinical environments, potentially through model compression or deployment via edge computing, to enable faster inference without sacrificing accuracy. Lastly, longitudinal studies that monitor the system's performance over time in real-world settings would offer valuable evidence regarding its reliability and clinical impact, ultimately supporting its integration into routine breast cancer screening programs.

## Conclusions

This study presents a novel approach to breast cancer detection using infrared thermographic images. By integrating convolutional neural networks (CNNs) with Enhanced Particle Swarm Optimization (EPSO) and Generative Adversarial Networks (GANs) for data augmentation, we have demonstrated a significant improvement in model performance, achieving a recognition rate of 98.8%. This result highlights the potential of combining advanced optimization techniques and synthetic data generation to enhance the accuracy and efficiency of cancer detection systems.

The proposed method shows great promise for improving the accuracy and speed of BC detection in clinical settings. The ability to automatically classify thermographic images with such high accuracy can aid radiologists and healthcare professionals in making faster, more reliable diagnoses. Given that the system is non-invasive, cost-effective, and easy to deploy, it could serve as an important tool for early detection, particularly in resource-limited settings where traditional diagnostic methods like mammography may not be accessible.

Additionally, the use of EPSO for optimizing CNN hyperparameters and GANs for data augmentation opens new avenues for improving medical image analysis techniques in general. This approach can be adapted for other types of medical imaging, such as X-rays, CT scans, or MRIs, offering potential for broader applications in healthcare diagnostics. The proposed system has several potential practical applications in the healthcare domain. First, it can be integrated into clinical workflows to assist radiologists in diagnosing breast cancer using thermographic images. This integration could serve as an alternative to conventional screening techniques, particularly in regions with limited access to mammography or ultrasound facilities. Additionally, due to its high classification accuracy, the system could be a valuable asset in early detection programs, helping to identify breast cancer at its initial stages and thereby enhancing treatment outcomes and patient survival rates. Furthermore, the non-invasive and cost-effective nature of thermography supports its implementation in telemedicine platforms, enabling remote diagnosis and consultations. This is especially beneficial in rural or underserved areas where access to specialized medical services may be limited.

## Data availability

**Data Availability Statement:** Breast Thermal images of patients of the Antonio Pedro University Hospital (HUAP), Brazil are publicly available in the Database for Mastology Research which stores and manages mastologic images of BC (accessed during 15 February – 15 August 2024). The data is publicly available at <https://visu.alic.uff.br/dmi/prontuario/home.php>. Dataset is published in Silva, L. F.; Saade, D. C. M.; Sequeiros, G. O.; Silva, A. C.; Paiva, A. C.; Bravo, R. S.; Conci, A., A New Database for Breast Research with Infrared Image, Journal of Medical Imaging and Health Informatics, Volume 4, Number 1, March 2014, pp. 92-100(9).

Received: 29 October 2024; Accepted: 8 July 2025

Published online: 13 July 2025

## References

1. Centers for Disease Control and Prevention. U.S. Cancer Statistics Lung Cancer Stat Bite. U.S. Department of Health and Human Services; (2024).

2. Sadeq Darrab, B. & Ergenc Vertical Pattern Mining Algorithm for Multiple Support Thresholds, Procedia Computer Science, Volume 112, Pages 417–426, ISSN 1877 – 0509, (2017). <https://doi.org/10.1016/j.procs.2017.08.051>
3. Spak, D. A., Plaxco, J. S., Santiago, L., Dryden, M. J. & Dogan, B. E. BI-RADS fifth edition: A summary of changes. *DiagnInterv Imaging.* **98** (3), 179–190. <https://doi.org/10.1016/j.diii.2017.01.001> (2017). Epub 2017 Jan 25. PMID: 28131457.
4. Hiba Asri, H., Mousannif, H. A., Moatassime, T. & Noel Using machine learning algorithms for breast Cancer risk prediction and diagnosis, procedia computer science, **83**, Pages 1064–1069, ISSN 1877 – 0509, (2016). <https://doi.org/10.1016/j.procs.2016.04.224>
5. Centers for Disease Control and Prevention. Incidence and Relative Survival by Stage at Diagnosis for Common Cancers; USCS Data Brief, n.A., GA: Centers for Disease Control and Prevention, US Department of Health and Human Services: Washington, DC, USA, (2021).
6. Kann, B. H., Hosny, A. & Aerts, H. J. W. L. Artificial intelligence for clinical oncology. *Cancer Cell.* **39** (7), 916–927. <https://doi.org/10.1016/j.ccr.2021.04.002> (2021). Epub 2021 Apr 29. PMID: 33930310; PMCID: PMC8282694.
7. Smith, J. et al. Advances in multimodal data integration for breast Cancer diagnosis. *Nat. Cancer Reviews.* **30** (1), 1–15. <https://doi.org/10.1038/s41568-023-00623-9> (2024).
8. Iqbal, M. S., Ahmad, W., Alizadehsani, R., Hussain, S. & Rehman, R. Breast Cancer dataset, classification and detection using deep learning. *Healthc. (Basel).* **10** (12), 2395. <https://doi.org/10.3390/healthcare10122395> (2022). PMID: 36553919; PMCID: PMC9778593.
9. Sarker, I. H. Machine learning: algorithms, Real-World applications and research directions. *SN Comput. Sci.* **2** (3), 160. <https://doi.org/10.1007/s42979-021-00592-x> (2021). Epub 2021 Mar 22. PMID: 33778771; PMCID: PMC7983091.
10. Kabiraj, S. et al. Breast Cancer Risk Prediction using XGBoost and Random Forest Algorithm, 2020 11th International Conference on Computing, Communication and Networking Technologies (ICCCNT), Kharagpur, India, 2020, pp. 1–4. <https://doi.org/10.1109/ICCCNT49239.2020.9225451>
11. Li, Q. et al. XGBoost-based and tumor-immune characterized gene signature for the prediction of metastatic status in breast cancer. *J. Transl. Med.* **20** (1), 177. <https://doi.org/10.1186/s12967-022-03369-9> (2022). PMID: 35436939; PMCID: PMC9014628.
12. Tseng, Y. J. et al. Predicting breast cancer metastasis by using serum biomarkers and clinicopathological data with machine learning technologies. *Int. J. Med. Inf.* **128**, 79–86 (2019). Epub 2019 May 7. PMID: 31103449.
13. Paik, E. S. et al. Prediction of survival outcomes in patients with epithelial ovarian cancer using machine learning methods. *J. Gynecol. Oncol.* **30** (4), e65. <https://doi.org/10.3802/jgo.2019.30.e65> (2019). Epub 2019 Mar 11. PMID: 31074247; PMCID: PMC6543110.
14. Altameem, A., Mahanty, C., Poonia, R. C., Saudagar, A. K. J. & Kumar, R. Breast Cancer detection in mammography images using deep convolutional neural networks and fuzzy ensemble modeling techniques. *Diagnostics* **12**, 1812. <https://doi.org/10.3390/diagnostics12081812> (2022).
15. Debendra Muduli, R., Dash, B., Majhi & Part, B. Automated diagnosis of breast cancer using multi-modal datasets: A deep convolution neural network based approach, Biomedical Signal Processing and Control, **71**, 1746–8094, <https://doi.org/10.1016/j.bspc.2021.102825>. (2022).
16. Wakili, M. A. et al. Classification of breast Cancer histopathological images using densenet and transfer learning. *ComputIntellNeurosci* **2022**, 8904768. <https://doi.org/10.1155/2022/8904768> (2022). PMID: 36262621; PMCID: PMC9576400.
17. Heenaye-Mamode Khan, M. et al. Multi- class classification of breast cancer abnormalities using deep convolutional neural network (CNN). *PLoS One.* **16** (8), e0256500. <https://doi.org/10.1371/journal.pone.0256500> (2021). PMID: 34437623; PMCID: PMC8389446.
18. Sakri, S. B., Abdul Rashid, N. B. & Muhammad Zain, Z. Particle Swarm Optimization Feature Selection for Breast Cancer Recurrence Prediction, in IEEE Access, vol. 6, pp. 29637–29647, (2018). <https://doi.org/10.1109/ACCESS.2018.2843443>
19. Mohan, S. & Mahesh, T. R. Particle Swarm Optimization based Contrast Limited enhancement for mammogram images, 2013 7th International Conference on Intelligent Systems and Control (ISCO), Coimbatore, India, 2013, pp. 384–388. <https://doi.org/10.1109/ISCO.2013.6481185>
20. Ibrahim, R., Ghnemat, R. & Abu Al-Haija, Q. Improving alzheimer's disease and brain tumor detection using deep learning with particle swarm optimization. *AI* **4**, 551–573. <https://doi.org/10.3390/ai4030030> (2023).
21. Karimi Jafarbigloo, S. & Danyali, H. Nuclear atypia grading in breast cancer histopathological images based on CNN feature extraction and LSTM classification. *CAAI Trans. Intell. Technol.* **6** (4), 426–439. <https://doi.org/10.1049/cit2.12061> (2021).
22. Kamel, S. R., YaghoubZadeh, R. & &Kheirabadi, M. Improving the performance of support-vector machine by selecting the best features by Gray Wolf algorithm to increase the accuracy of diagnosis of breast cancer. *J. Big Data.* **6**, 90. <https://doi.org/10.1186/s40537-019-0247-7> (2019).
23. Lahoura, V. et al. Cloud Computing-Based framework for breast Cancer diagnosis using extreme learning machine. *Diagnostics* **11**, 241. <https://doi.org/10.3390/diagnostics11020241> (2021).
24. Jakhar, A. K., Gupta, A. & Singh, M. SELF: a stacked-based ensemble learning framework for breast cancer classification. *Evol. Intel.* **17**, 1341–1356. <https://doi.org/10.1007/s12065-023-00824-4> (2024).
25. Nawaz, M., Sewissy, A. A. & Soliman, T. H. A. Multi-class breast cancer classification using deep learning convolutional neural network. *Int. J. Adv. Comput. Sci. Appl. (IJACSA).* **9** (6), 316–322 (2018).
26. Supriya, M. & Deepa, A. J. A novel approach for breast cancer predictions using optimized ANN classifiers based on big data environment. *Health Care Manag Sci.* **23** (3), 414–426 (2020).
27. Görgel, P., Sertbas, A. & Ucan, O. N. Mammographical mass detection and classification using local seed region growing-spherical wavelet transform (LSRG-SWT) hybrid scheme. *Comput. Biol. Med.* **43** (6), 765–774 (2013). Epub 2013 Mar 27. PMID: 23668353.
28. Iqbal, M. S., Ahmad, W., Alizadehsani, R., Hussain, S. & Rehman, R. *Breast Cancer Dataset, Classification and Detection Using Deep Learning102395* (Healthcare, 2022).
29. Berbar, M. A., Reyad, Y. A. & Hussain, M. Breast Mass Classification using Statistical and Local Binary Pattern Features, 16th International Conference on Information Visualisation, Montpellier, France, 2012, pp. 486–490. <https://doi.org/10.1109/IV.2012.84>
30. Zhang, S. et al. Potential rapid intraoperative cancer diagnosis using dynamic full-field optical coherence tomography and deep learning: A prospective cohort study in breast cancer patients. *Sci. Bull.* **69** (Issue 11), 1748–1756. <https://doi.org/10.1016/j.scib.2024.03.061> (2024).
31. Silva, L. F. et al. A New Database for Breast Research with Infrared Image, Journal of Medical Imaging and Health Informatics, Volume 4, Number 1, March pp. 92–100(9). (2014).
32. Silva, L. F. et al. Hybrid analysis for indicating patients with breast cancer using temperature time series. *Comput. Methods Programs Biomed.* **130**, 142–153. <https://doi.org/10.1016/j.cmpb.2024.03.061> (2016).
33. Russo, F. Edge detection in noisy images using fuzzy reasoning, IMTC/98 Conference Proceedings. IEEE Instrumentation and Measurement Technology Conference. Where Instrumentation is Going (Cat. No.98CH36222), St. Paul, MN, USA, pp. 369–372 vol.1, (1998). <https://doi.org/10.1109/IMTC.1998.679808>
34. Mario Versaci and Francesco Carlo Morabito Image Edge Detection. A new approach based on fuzzy entropy and fuzzy divergence. *Int. J. Fuzzy Syst.* **23** (4), 918–936 (2021).
35. Melin, P., Gonzalez, C. I., Castro, J. R., Mendoza, O. & Castillo, O. Edge-Detection method for image processing based on generalized Type-2 fuzzy logic. *IEEE Trans. Fuzzy Syst.* **22** (6), 1515–1525. <https://doi.org/10.1109/TFUZZ.2013.2297159> (Dec. 2014).
36. Verma, O. P. & Parihar, A. S. An optimal fuzzy system for edge detection in color images using bacterial foraging algorithm. *IEEE Trans. Fuzzy Syst.* **25** (1), 114–127. <https://doi.org/10.1109/TFUZZ.2016.2551289> (Feb. 2017).

37. Eberhart, R. C. & Kennedy, J. A new optimizer using particle swarm theory. Proceedings of the Sixth International Symposium on Micromachine and Human Science, Nagoya, Japan. pp. 39–43, (1995).
38. Kennedy, J. & Eberhart, R. C. Particle swarm optimization. Proceedings of IEEE International Conference on Neural Networks, Piscataway, NJ. pp. 1942–1948, (1995).
39. Wu, H. T., Huang, J. & Shi, Y. Q. A reversible data hiding method with contrast enhancement for medical images. *J. Vis. Communun. Image Represent.* **31** <https://doi.org/10.1016/j.jvcir.2015.06.010> (2015). Pages 146–153, ISSN 1047–3203.
40. Fang, J. L. T. F., Wang, X., Echizen, I., Yamagishi, J. & Kinnunen, T. Can we steal your vocal identity from the Internet? Initial investigation of cloning Obama's voice using GAN, WaveNet and low-quality found data, arXiv:1803.00860.
41. Eirikur Agustsson, M., Tschanne, F., Mentzer, R., Timofte, L. & Van Gool Generative Adversarial Networks for Extreme Learned Image Compression, arXiv:180402958
42. Arjovsky, M., Chintala, S. & Bottou, L. and Wasserstein Generative Adversarial Networks. In Proceedings of the 34th International Conference on Machine Learning (ICML)2017, pp. 214–223.
43. Furdui, A., Zhang, T., Worring, M., Cesar, P. & Abdallah El, A. AC-WGAN-GP: Augmenting ECG and GSR Signals using Conditional Generative Models for Arousal Classification. In Adjunct Proceedings of the 2021 ACM International Joint Conference on Pervasive and Ubiquitous Computing and Proceedings of the 2021 ACM International Symposium on Wearable Computers (UbiComp/ISWC '21 Adjunct). Association for Computing Machinery, New York, NY, USA, 21–22. (2021). <https://doi.org/10.1145/3460418.3479301>
44. Zhang, Y., Liu, H., Wang, X. & Chen, J. Deep convolutional neural network for breast Cancer classification using infrared thermal images. *IEEE Access.* **10**, 32645–32656. <https://doi.org/10.1109/ACCESS.2022.3157432> (2022).
45. Rojas, M., Naranjo-Torres, J. & Meneses, J. Breast cancer detection using thermal images and deep learning. In H. Florez & S. Misra (Eds.), Applied Informatics: Fourth International Conference, ICAI 2021 (pp. 428–440). Springer, (2021). [https://doi.org/10.1007/978-3-030-89654-6\\_30](https://doi.org/10.1007/978-3-030-89654-6_30)
46. Bohlouri, M., Keyvanpour, M. R. & Vahab Shojaedini, S. Enhancing Breast Cancer Detection from Thermographic Images: A Hybrid Approach Using Transfer Learning and Generative Adversarial Networks, 2024 10th International Conference on Web Research (ICWR), Tehran, Iran, Islamic Republic of, pp. 27–31, (2024). <https://doi.org/10.1109/ICWR61162.2024.10533359>
47. Shobhana Periyasamy, A., Prakasaraao, M., Menaka, B., Venkatraman, M. & Jayashree Support vector machine based methodology for classification of thermal images pertaining to breast cancer. *J. Therm. Biology Volume.* **110**, 103337. <https://doi.org/10.1016/j.jtherbio.2022.103337> (2022).
48. Karaman, A. et al. Hyper-parameter optimization of deep learning architectures using artificial bee colony (ABC) algorithm for high performance real-time automatic colorectal cancer (CRC) polyp detection. *Appl. Intell.* **53**, 15603–15620 (2023).
49. Ahmet Karaman, I. et al. Robust real-time polyp detection system design based on YOLO algorithms by optimizing activation functions and hyper-parameters with artificial bee colony (ABC), expert systems with applications, 221, 2023, 119741, ISSN 0957–4174, <https://doi.org/10.1016/j.eswa.2023.119741>
50. Bayram, B., Kunduracioglu, I., Ince, S. & Pacal, I. A systematic review of deep learning in MRI-based cerebral vascular occlusion-based brain diseases. *Neuroscience.* ;568:76–94. (2025). <https://doi.org/10.1016/j.neuroscience.2025.01.020>. Epub 2025 Jan 11. PMID: 39805420.
51. Burhanettin Ozdemir, I. & Pacal An innovative deep learning framework for skin cancer detection employing ConvNeXtV2 and focal self-attention mechanisms, results in engineering, 25, 2025, 103692, ISSN 2590 – 1230, <https://doi.org/10.1016/j.rineng.2024.103692>
52. İşik, G. & Paçal, İ. Few-shot classification of ultrasound breast cancer images using meta-learning algorithms. *Neural Comput. Applic.* **36**, 12047–12059. <https://doi.org/10.1007/s00521-024-09767-y> (2024).

## Author contributions

R.M.A., and M.Y.S proposed the main idea. S.B.S, M.A, A.F.S, A.A and S.S.B. checked and discussed the results and the whole manuscript. P.N.B and E.Y.K.N contributed to the discussion of this study. All authors have approved the final version of this manuscript.

## Funding

This research was funded by the Deanship of Postgraduate Studies and Scientific Research at Majmaah University through the project number ICR-2025-1879.

## Declarations

### Competing interests

The authors declare no competing interests.

### Additional information

**Correspondence** and requests for materials should be addressed to M.Y.S.

**Reprints and permissions information** is available at [www.nature.com/reprints](http://www.nature.com/reprints).

**Publisher's note** Springer Nature remains neutral with regard to jurisdictional claims in published maps and institutional affiliations.

**Open Access** This article is licensed under a Creative Commons Attribution-NonCommercial-NoDerivatives 4.0 International License, which permits any non-commercial use, sharing, distribution and reproduction in any medium or format, as long as you give appropriate credit to the original author(s) and the source, provide a link to the Creative Commons licence, and indicate if you modified the licensed material. You do not have permission under this licence to share adapted material derived from this article or parts of it. The images or other third party material in this article are included in the article's Creative Commons licence, unless indicated otherwise in a credit line to the material. If material is not included in the article's Creative Commons licence and your intended use is not permitted by statutory regulation or exceeds the permitted use, you will need to obtain permission directly from the copyright holder. To view a copy of this licence, visit <http://creativecommons.org/licenses/by-nc-nd/4.0/>.

© The Author(s) 2025, corrected publication 2025